

# Discretization of continuous-time arbitrage strategies in financial markets with fractional Brownian motion

Kerstin Lamert · Benjamin R. Auer · Ralf Wunderlich

Version of December 25, 2024

**Abstract** This study evaluates the practical usefulness of continuous-time arbitrage strategies designed to exploit serial correlation in fractional financial markets. Specifically, we revisit the strategies of Shiryaev (1998) and Salopek (1998) and transfer them to a real-world setting by discretizing their dynamics and introducing transaction costs. In Monte Carlo simulations with various market and trading parameter settings as well as a formal analysis of discretization error, we show that both are promising with respect to terminal portfolio values and loss probabilities. These features and complementary sparsity make them worth serious consideration in the toolkit of quantitative investors.

**Keywords** Arbitrage strategies; fractional Brownian motion; fractional Black-Scholes model; serial correlation; simulation

**Mathematics Subject Classification (2010)** 91G10 · 91G80

**JEL classification** G11 · G17

## 1 Introduction

Motivated by the challenge they pose to the traditional notion of efficient capital markets, financial research has intensively studied investment strategies which solely rely on past asset price information (see Goyal and Jegadeesh, 2018). Among the most prominent studies, Jegadeesh and Titman (1993, 2001) have shown that cross-sectional momentum, i.e., buying past winners and selling past losers, is highly beneficial.<sup>1</sup> In addition, Moskowitz et al. (2012) identify a time-series momentum effect according to which single assets ex-

---

Kerstin Lamert

Brandenburg University of Technology Cottbus-Senftenberg, Institute of Mathematics, Platz der Deutschen Einheit 1, 03046 Cottbus, Germany; E-mail: kerstin.lamert@b-tu.de

Benjamin R. Auer

Friedrich Schiller University Jena, Chair of Finance, Carl-Zeiss-Str. 3, 07743 Jena, Germany; E-mail: benjamin.auer@uni-jena.de

Ralf Wunderlich

Brandenburg University of Technology Cottbus-Senftenberg, Institute of Mathematics, Platz der Deutschen Einheit 1, 03046 Cottbus, Germany; E-mail: ralf.wunderlich@b-tu.de

<sup>1</sup> For the identification of winners and losers, relative past performance can be quantified via cumulative returns or established reward-to-risk performance measures (see Rachev et al., 2007).

hibit exploitable trending behavior.<sup>2</sup> What these strategies have in common is that their profitability is linked to a positive serial correlation in asset price movements (see Pan et al., 2004; Hong and Satchell, 2015).

Even though momentum investing has become a standard in the mutual fund industry (see Barroso and Santa-Clara, 2015), financial research and practice has paid surprisingly little attention to a very interesting strand of mathematical literature developing arbitrage strategies for assets with serially correlated returns. It is well known that *pure arbitrage*, i.e., the realization of risk-less profits from zero initial investment, is impossible in a traditional Black-Scholes market with standard Brownian motion (sBm). In contrast, arbitrage opportunities can arise in markets where asset prices are driven by a fractional Brownian motion (fBm) which dates back to Mandelbrot and Ness (1968) and superimposes memory features on asset returns. In a continuous-time setup with slowly decaying positive serial correlation, i.e., the fractional Black-Scholes model of Cutland et al. (1995), the theoretical studies of Shiryaev (1998) and Salopek (1998) show that risk-less profits can be earned by buying high-priced and short-selling low-priced assets in adequate numbers. Bayraktar and Poor (2005) extend the work of Shiryaev (1998) by incorporating stochastic volatility. Rogers (1997) and Cheridito (2003) develop additional but more complex strategies.

While the simplicity of the Shiryaev and Salopek arbitrage strategies and empirical evidence on memory in equity, futures and fund returns (see Wang et al., 2012; Di Cesare et al., 2015; Coakley et al., 2016) make them appealing for investment practice, they are built on the premise of continuous-time trading with no frictions. Cheridito (2003) and Guasoni (2006) highlight that, in a fractional Black-Scholes world, arbitrage opportunities vanish with the introduction of a minimal waiting time between subsequent transactions, i.e., discrete-time trading, and proportional transaction costs of any positive size, respectively.<sup>3</sup> However, this does not necessarily mean that the above strategies should be discarded. When suitably discretized and parameterized, they may not be entirely self-financing and risk-free, but still provide positive expected payoffs at a low risk of loss. In other words, they could share some valuable properties with *statistical arbitrage* strategies (see Bondarenko, 2003; Lütkebohmert and Sester, 2019). Just recently, two interesting strategies of this kind have been proposed to exploit fBm market behavior. Garcin (2022) enters (long or short) trading positions by explicitly forecasting future realizations of the fBm, whereas Xiang and Deng (2024) construct a (long-only) buy-and-hold strategy with growing stop-profit boundary. However, both strategies involve tuning a variety of parameters. In addition, the former requires more than just current prices to derive an investment decision and the latter only benefits from rising asset prices. As we will see, these are limitations compared to the simpler yet more flexible strategies we focus on.

The goal of our study is straightforward. After exploring the properties and the economic intuition of the Shiryaev and Salopek strategies, the core objective of our study is to investigate their investment performance in a real-world setting. This means that, in a first step, we discretize the strategies and install different forms of transaction costs. This is not trivial because discretization alone makes the strategies lose their self-financing property

<sup>2</sup> Marshall et al. (2017) establish a connection between time-series momentum and the popular moving average trading rules of Brock et al. (1992). Zakamulin and Giner (2024) uncover the price processes under which more general moving average rules perform best.

<sup>3</sup> Peyre (2017) shows that certain simple strategies (i.e., linear combinations of buy-and-hold investments with regular rebalancing) do not generate any arbitrage profits even if there is no minimal waiting time between trades. For research on the role of other frictions, see Guasoni et al. (2019, 2021).

and requires suitable countermeasures to maintain tradeability. In a second step, we perform an extensive Monte Carlo study for the discretized versions of the strategies. Here, we are particularly interested in whether they deliver positive terminal portfolio values on average and display acceptably small loss probabilities. We focus on these two quantities because they are central to established arbitrage definitions and allow a modern downside-oriented investment evaluation (see Eling and Schuhmacher, 2007; Cumova and Nawrocki, 2014). To answer our research question, we use the circulant embedding method of Wood and Chan (1994) for fBm simulation which, in contrast to alternatives, preserves the basic features of fBms and shines by remarkable computation speed (see Coeurjolly, 2000; Kijima and Tam, 2013). We analyze the strategies with asset and trading parameters tailored to the current market environment exhibiting, for example, significantly falling transaction costs (see Chordia et al., 2014). Furthermore, we conduct a variety of sensitivity checks to identify the situations in which they perform best and worst. This and a supplementary formal inspection of discretization error result in an intuitive guide on how to choose, for example, the ideal candidate assets, parameters and trading frequencies of the strategies.

The remainder of our study is organized as follows. Section 2 introduces the fractional Black-Scholes model, discusses the corresponding Shiryaev and Salopek arbitrage strategies and translates them to a discrete-time setting with transaction costs. Section 3 presents our Monte Carlo study examining the impact of discretization, transaction costs, model parameters as well as trading horizon and frequency on the strategies. Section 4 illustrates empirical implementation issues by applying them to an exemplary data set of emerging market stocks. Section 5 concludes and outlines directions for future research.

## 2 Theoretical framework

### 2.1 Continuous-time market setup

We start our analysis by specifying the asset price behavior in a fractional Black-Scholes model and explain how self-financing portfolios are formed in such an environment.

**Asset prices.** For a fixed date or investment horizon  $T > 0$ , we consider a filtered probability space  $(\Omega, \mathcal{F}, \mathbb{F}, \mathbb{P})$  with standard filtration  $\mathbb{F} = (\mathcal{F}_t)_{t \in [0, T]}$  and assume that all processes are  $\mathbb{F}$ -adapted. In this context, the *fractional Black-Scholes model* suggests that we have one risk-free asset with constant price  $S_t^0 = 1$  and  $d$  risky assets with a price process  $S = (S^1, \dots, S^d)$  defined on  $[0, T]$  by the stochastic differential equations (SDEs)

$$dS_t^i = \mu^i S_t^i dt + \sigma^i S_t^i dB_t^{H^i}, \quad S_0^i = s_0^i, \quad i = 1, \dots, d. \quad (2.1)$$

Here, the drifts or expected returns  $\mu^i \in \mathbb{R}$ , volatilities  $\sigma^i > 0$  and initial prices  $s_0^i > 0$  are given constants. In contrast to the standard Black-Scholes model, the SDEs are not driven by sBms (or Wiener processes) but by fBms  $B_t^{H^i}$  with Hurst parameters  $H^i \in (0.5, 1)$ . The fBms are assumed to be independent, which is reasonable when the risky assets are, for example, certain types of industry portfolios, investment funds or commodity futures baskets (see Erb and Harvey, 2006; Badrinath and Gubellini, 2011).<sup>4</sup>

<sup>4</sup> A formal discussion of correlated fBms can be found in Amblard et al. (2013).

The one-dimensional fBm  $(B_t^H)_{t \in [0, T]}$  is a centered Gaussian process with covariance

$$\text{Cov}(B_t^H, B_s^H) = \frac{1}{2} (|t|^{2H} + |s|^{2H} - |t-s|^{2H}) \quad \text{for } H \in (0, 1). \quad (2.2)$$

It is a self-similar process with stationary increments. The special case  $H = 0.5$  reflects the sBm which has independent increments and enjoys the martingale property. For  $H \neq 0.5$ , the increments are correlated and the process is not a martingale. This implies memory effects for the asset returns  $dS_t^i/S_t^i$ . For the range  $H \in (0.5, 1)$  considered in the fractional Black-Scholes world, asset returns are positively correlated, i.e., persistent. While, for  $H = 0.5$ , we have to rely on Itô's calculus,  $H > 0.5$  allows us to define stochastic integrals w.r.t.  $B_t^H$  path-wise in the Riemann-Stieltjes sense (see Sottinen and Valkeila, 2003). Thus, the solutions of the SDEs in (2.1) are

$$S_t^i = s_0^i \exp \{ \mu^i t + \sigma^i B_t^{H^i} \}, \quad t \in [0, T]. \quad (2.3)$$

The processes defined in (2.3) are called geometric fBms.<sup>5</sup>

**Portfolios.** Asset transactions in a fractional Black-Scholes market are modeled based on the usual assumptions of permanent trading, unlimited borrowing and short-selling, real asset quantities and contemporary agreement of buying and selling prices. Furthermore, we assume that trades do not affect market prices and, at this point, there are no transaction costs, fees or taxes. We can describe the trading activity of an investor by an initial amount of capital  $v \in \mathbb{R}$  and a  $\mathbb{F}$ -adapted process

$$\Psi = (\Psi_t)_{t \in [0, T]} = (\Psi_t^0, \Psi_t^1, \dots, \Psi_t^d)_{t \in [0, T]}. \quad (2.4)$$

Here,  $\Psi_t^0 \in \mathbb{R}$  and  $\Psi_t^1, \dots, \Psi_t^d \in \mathbb{R}$  denote the numbers of risk-free and risky assets held by the investor at time  $t$ , respectively.  $\Psi$  is called *portfolio* or *trading strategy*. The investor has a long (short) position if  $\Psi_t^i, i = 0, \dots, d$ , is positive (negative). At time  $t$ , the value  $V_t^\Psi$  of the portfolio  $\Psi$  is given by

$$V_t^\Psi = \sum_{i=0}^d \Psi_t^i S_t^i. \quad (2.5)$$

$V^\Psi = (V_t^\Psi)_{t \in [0, T]}$  is the *value process* of  $\Psi$ . In an arbitrage context,  $\Psi$  is assumed to be *self-financing*. This means that there is no exogenous infusion or withdrawal of capital after the purchase of the portfolio. Rebalancing the portfolio must be financed solely by trading the  $d + 1$  available assets. Mathematically, self-financing in a continuous-time market is defined by the property that the value process for all  $t \in [0, T]$  can be expressed as

$$V_t^\Psi = v + G_t^\Psi, \quad \text{where } G_t^\Psi = \sum_{i=0}^d \int_0^t \Psi_s^i dS_s^i. \quad (2.6)$$

$G^\Psi = (G_t^\Psi)_{t \in [0, T]}$  is the *gain process* of  $\Psi$ , where the gain  $G_t^\Psi$  at time  $t$  is given by a sum of stochastic integrals w.r.t. geometric fBms (see Salopek, 1998).<sup>6</sup> The self-financing condition (2.6) can also be stated in differential form, i.e.,  $dV_t^\Psi = \sum_{i=0}^d \Psi_t^i dS_t^i$ . It shows that, for a self-financing strategy, the changes in portfolio value are not due to rebalancing but rather to changes in asset prices.

<sup>5</sup> For the sBm with  $H^i = 0.5$ , we have  $S_t^i = s_0^i \exp \{ (\mu^i - (\sigma^i)^2/2)t + \sigma^i B_t^{H^i} \}$ . Properties of fBms and the associated integration theory are outlined in Biagini et al. (2008), Mishura (2008) and Bender et al. (2011).

<sup>6</sup> Here, it is crucial to apply forward or Riemann-Stieltjes integrals because alternative stochastic integral definitions contradict economic intuition (see Hu and Øksendal, 2003; Rostek and Schöbel, 2013).

## 2.2 Continuous-time arbitrage

In a standard Black-Scholes world, arbitrage is impossible. This is a consequence of the fundamental theorem of asset pricing (see Delbaen and Schachermayer, 1994; Björk, 2004) and has its roots in the sBm martingale property. In contrast, a fBm with  $H \neq 0.5$  behaves predictably such that our fractional Black-Scholes world offers arbitrage opportunities which can be exploited by constructing suitable arbitrage portfolios. A self-financing portfolio  $\Psi$  is called an *arbitrage portfolio* if its value process satisfies

$$\begin{aligned} \text{(i)} \quad & V_0^\Psi = 0, \\ \text{(ii)} \quad & \mathbb{P}(V_t^\Psi \geq -\underline{v} \text{ for all } t \in (0, T]) = 1, \text{ for some constant } \underline{v} \geq 0, \\ \text{(iii)} \quad & \mathbb{P}(V_T^\Psi \geq 0) = 1 \text{ and } \mathbb{P}(V_T^\Psi > 0) > 0. \end{aligned} \quad (2.7)$$

This implies that arbitrage is essentially the possibility to generate a positive amount of money without having to invest any initial capital and without any risk of loss. The value of the arbitrage portfolio is bounded from below at all times and non-negative at the end of the investment horizon.<sup>7</sup> In the following, we present two simple arbitrage strategies satisfying all three properties in (2.7) with  $\underline{v} = 0$ . That is, their portfolio values never fall below zero.

**Remark 2.1** For every arbitrage strategy  $\Psi$ , the scaled strategy  $\tilde{\Psi} = \gamma\Psi$  with  $\gamma > 0$  is also an arbitrage strategy. This is because (2.5) and (2.6) imply  $V^{\tilde{\Psi}} = \gamma V^\Psi$  and  $G^{\tilde{\Psi}} = \gamma G^\Psi$ , respectively. Since the initial value  $V_0^\Psi$  is zero, we also have  $V_0^{\tilde{\Psi}} = 0$ . Hence,  $\tilde{\Psi}$  satisfies the self-financing condition  $V_t^{\tilde{\Psi}} = v + G_t^{\tilde{\Psi}}$  in (2.6) with  $v = 0$ . Finally,  $V^{\tilde{\Psi}} = \gamma V^\Psi$  implies that  $\tilde{\Psi}$  fulfills the arbitrage conditions in (2.7).

**Shiryaev strategy.** Shiryaev (1998) proposes a strategy that generates an arbitrage portfolio consisting of the risk-free asset and one risky asset.<sup>8</sup> Thus, we have  $d = 1$ . For simplicity, we denote the drift, volatility and Hurst coefficient of the risky asset by  $\mu$ ,  $\sigma$  and  $H$ , respectively. For the two assets, the strategy suggests entering the time  $t \in [0, T]$  positions

$$\begin{aligned} \Psi_t^0 &= \frac{1}{s_0^1} ((s_0^1)^2 - (S_t^1)^2) = s_0^1 (1 - \exp\{2\mu t + 2\sigma B_t^H\}), \\ \Psi_t^1 &= \frac{2}{s_0^1} (S_t^1 - s_0^1) = 2(\exp\{\mu t + \sigma B_t^H\} - 1). \end{aligned} \quad (2.8)$$

At every  $t$ , it compares the value  $S_t^1$  of a pure risky investment with an alternative investment of the initial risky asset price  $s_0^1$  in the risk-free asset. Because, in our market model, we have  $S_t^0 = 1$ , this alternative investment has a constant value of  $s_0^1$ .<sup>9</sup> If the value  $S_t^1$  of the pure risky investment exceeds (falls below) the value  $s_0^1$  of the alternative investment, the investor holds a long (short) position in the risky asset and a short (long) position in the risk-free asset. In the case of equality, he is not invested and the portfolio value is zero. The number of risky asset shares  $\Psi_t^1$  in (2.8) does not depend on the initial risky asset price  $s_0^1$  but on the parameters  $\mu$ ,  $\sigma$  and  $H$ .

<sup>7</sup> A negative lower bound rules out so-called doubling-type arbitrage strategies. Portfolios satisfying (i) to (iii) are also referred to as nds-admissible (no doubling strategies) arbitrages (see Bender et al., 2011).

<sup>8</sup> In an independent study, the same strategy has been derived by Dasgupta and Kallianpur (2000).

<sup>9</sup> The strategy can be easily generalized to markets with risk-free asset prices  $S_t^0 = e^{rt}$ , where  $r \geq 0$  denotes the risk-free rate (see Shiryaev, 1998).

Shiryaev (1998) shows that the strategy  $\Psi$  in (2.8) is self-financing. Furthermore, at time  $t = 0$ , we have  $\Psi_0^0 = \Psi_0^1 = 0$  and hence  $V_0^\Psi = 0$ , i.e., no initial investment is required. Substituting (2.8) into (2.5) shows that the portfolio value at any time  $t \in [0, T]$  is

$$V_t^\Psi = (S_t^1 - s_0^1)^2 / s_0^1 \geq 0. \quad (2.9)$$

Thus, condition (ii) in (2.7) holds with the lower bound  $\underline{v} = 0$ . We also obtain  $\mathbb{P}(V_T^\Psi \geq 0) = 1$  and  $\mathbb{P}(V_T^\Psi > 0) > 0$ . This shows that  $\Psi$  is indeed an arbitrage strategy.

Relation (2.9) and the fact that the asset price  $S_t^1$  is lognormally distributed allow us to derive the following closed-form expressions for the distribution of the terminal wealth  $V_T^\Psi$  and its parameters.

**Proposition 2.1 (Distribution of the terminal Shiryaev portfolio value)** *The mean of the terminal portfolio value  $V_T^\Psi$  of the continuous-time Shiryaev strategy is given by*

$$\mathbb{E}[V_T^\Psi] = s_0^1 (g(2\mu T, 4\sigma^2 T^{2H}) - 2g(\mu T, \sigma^2 T^{2H}) + 1), \quad (2.10)$$

where  $g(m, \Sigma) = \exp\{m + \Sigma/2\}$  is the mean of a lognormally distributed random variable with parameters  $m$  and  $\Sigma$ . For the variance, we have  $\text{Var}(V_T^\Psi) = \mathbb{E}[(V_T^\Psi)^2] - (\mathbb{E}[V_T^\Psi])^2$  with the second-order moment

$$\begin{aligned} \mathbb{E}[(V_T^\Psi)^2] &= (s_0^1)^2 (g(4\mu T, 16\sigma^2 T^{2H}) - 4g(3\mu T, 9\sigma^2 T^{2H}) \\ &\quad + 6g(2\mu T, 4\sigma^2 T^{2H}) - 4g(\mu T, \sigma^2 T^{2H}) + 1). \end{aligned}$$

The cumulative distribution function of  $V_T^\Psi$  is

$$\begin{aligned} F_{V_T^\Psi}(v) = \mathbb{P}(V_T^\Psi \leq v) &= \bar{\Phi}\left(\frac{1}{\sigma T^H} \left(\log\left\{1 + \sqrt{v/s_0^1}\right\} - \mu T\right)\right) \\ &\quad - \bar{\Phi}\left(\frac{1}{\sigma T^H} \left(\log\left\{\left(1 - \sqrt{v/s_0^1}\right)^+\right\} - \mu T\right)\right), \quad v \geq 0, \end{aligned}$$

where  $\bar{\Phi}$  denotes the cumulative distribution function of the standard normal distribution,  $x^+ = \max(x, 0)$  for  $x \in \mathbb{R}$ , and  $\log 0$  is set to  $-\infty$ .

*Proof.* See Appendix A.1.

**Salopek strategy.** Another arbitrage strategy, dating back to Harrison et al. (1984) and applied in a fractional Black-Scholes market by Salopek (1998), trades  $d \geq 2$  risky assets and ignores the risk-free asset. It is defined for two real-valued constants  $\alpha < \beta$  and can be summarized as  $\Psi = (0, \Psi(\alpha, \beta))$  or, with some abuse of notation,  $\Psi = \Psi(\alpha, \beta)$ . The entries of  $\Psi(\alpha, \beta) = (\Psi_t^1(\alpha, \beta), \dots, \Psi_t^d(\alpha, \beta))$  are the risky asset shares at time  $t \in [0, T]$ . Specifically, for  $i = 1, \dots, d$ , we have

$$\Psi_t^i(\alpha, \beta) = \widehat{\Psi}_t^i(\beta) - \widehat{\Psi}_t^i(\alpha), \quad \text{where} \quad \widehat{\Psi}_t^i(a) = \frac{1}{d} \left( \frac{S_t^i}{M_a(S_t)} \right)^{a-1}. \quad (2.11)$$

$M_a(x)$  denotes the  $a$ -order power mean of  $x = (x^1, \dots, x^d) \in \mathbb{R}_+^d$ . It is given by

$$\begin{aligned} M_a(x) &= \left( \frac{1}{d} \sum_{i=1}^d (x^i)^a \right)^{1/a} \quad \text{for } a \neq 0, \\ M_0(x) &= \sqrt[d]{x^1 \cdot \dots \cdot x^d} \quad \text{for } a = 0. \end{aligned} \quad (2.12)$$

To provide an economic interpretation of this strategy, it is instructive to recall some properties of the involved family of power means (see Hardy et al., 1934).

**Remark 2.2** *With respect to the properties of the  $a$ -order power mean, we can list the following important special cases:*

$$\begin{aligned}
M_1(x) &= (x^1 + \dots + x^d)/d && \text{(arithmetic mean)} \\
M_2(x) &= \sqrt{((x^1)^2 + \dots + (x^d)^2)/d} && \text{(quadratic mean)} \\
M_{-1}(x) &= ((1/x^1 + \dots + 1/x^d)/d)^{-1} && \text{(harmonic mean)} \\
M_0(x) &= \sqrt[d]{x^1 \cdot \dots \cdot x^d} = \lim_{a \rightarrow 0} M_a(x) && \text{(geometric mean)} \\
M_\infty(x) &:= \lim_{a \rightarrow +\infty} M_a(x) = x_{\max} = \max\{x^1, \dots, x^d\} && \text{(maximum of } x) \\
M_{-\infty}(x) &:= \lim_{a \rightarrow -\infty} M_a(x) = x_{\min} = \min\{x^1, \dots, x^d\} && \text{(minimum of } x)
\end{aligned}$$

Furthermore, the function  $a \mapsto M_a(x)$  is increasing. For  $a < b$ , we have

$$x_{\min} \leq M_a(x) \leq M_b(x) \leq x_{\max} \quad (2.13)$$

with equalities if and only if  $x^1 = \dots = x^d = \bar{x}$ , i.e., all entries of  $x$  are identical. In this situation,  $M_a(x) = \bar{x}$  holds for all  $a \in \mathbb{R}$ .

The strategy  $\Psi(\alpha, \beta)$  in (2.11) is expressed as the difference between  $\widehat{\Psi}(\beta)$  and  $\widehat{\Psi}(\alpha)$ . Because these two components can be considered as strategies themselves, we call  $\widehat{\Psi}(a)$  an  $a$ -strategy or  $a$ -portfolio. Consequently, an investor can implement  $\Psi(\alpha, \beta)$  by purchasing a  $\beta$ -portfolio and short-selling an  $\alpha$ -portfolio.

Substituting the  $\widehat{\Psi}(a)$  specified by (2.11) into (2.5) provides the portfolio value of an  $a$ -strategy, i.e., we obtain

$$V_t^{\widehat{\Psi}(a)} = M_a(S_t). \quad (2.14)$$

It also shows that  $V_0^{\widehat{\Psi}(a)} = M_a(s_0)$ , i.e., the initial investment is positive and equals the  $a$ -order power mean of initial asset prices  $s_0$ . An  $a$ -strategy investor enters long positions in all  $d$  risky assets and chooses their numbers proportional to  $(S_t^i)^{a-1}$ . More specifically, for  $a = 1$ , we have  $\widehat{\Psi}_t^i = 1/d$ , i.e., an equally allocated investment, and the portfolio value is  $V_t^{\widehat{\Psi}(1)} = M_1(S_t)$ , i.e., the arithmetic mean of prices. For  $a > 1$  ( $a < 1$ ), the portfolio contains more (fewer) high-priced assets than low-priced assets. This feature becomes more pronounced with higher (lower) orders  $a > 1$  ( $a < 1$ ). In the limit for  $a \rightarrow \infty$  ( $a \rightarrow -\infty$ ), the investor only holds the asset with the highest (lowest) price. If there are  $m \geq 1$  risky assets sharing this price, he orders  $1/m$  each.

The strategy (2.11) is an arbitrage strategy if we impose the following assumption on the financial market model.

**Assumption 2.1** *All price processes  $(S_t^i)_{t \in [0, T]}$  of the risky assets  $i = 1, \dots, d$  start at time  $t = 0$  with identical initial prices  $S_0^i = \tilde{s} > 0$ .*

**Remark 2.3** *Assumption 2.1 serves mathematical simplification and will not be fulfilled in practice. However, this is not problematic because we can rescale the asset prices via  $\tilde{S}_t^i = \frac{\tilde{s}}{S_0^i} S_t^i$  to  $\tilde{S}_0^i = \tilde{s}$  and compute the arbitrage positions  $\tilde{\Psi}_t^i$  in the rescaled market. They are linked to the original market via  $\Psi_t^i = \frac{\tilde{s}}{S_0^i} \tilde{\Psi}_t^i$ . Because  $\Psi_t^i S_t^i = \tilde{\Psi}_t^i \tilde{S}_t^i$ , (2.5) delivers  $V_t^\Psi = V_t^{\tilde{\Psi}}$ . That is, the portfolio value is not affected by the transformation.*

We now show that (2.11) satisfies the three conditions in (2.7) and is in fact an arbitrage strategy. As far as the self-financing property is concerned, it has been verified by Salopek (1998). According to (2.14), for all  $t \in [0, T]$ , the portfolio value is given by

$$V_t^\Psi = V_t^{\hat{\Psi}(\beta)} - V_t^{\hat{\Psi}(\alpha)} = M_\beta(S_t) - M_\alpha(S_t) \geq 0, \quad (2.15)$$

where we have used the assumption  $\alpha < \beta$  and relation (2.13) stating that  $M_a(\cdot)$  is increasing in  $a$ . This proves condition (ii) in (2.7) with the lower bound  $\underline{v} = 0$ . Condition (i) on zero initial investment follows from Assumption 2.1 of identical initial asset prices. It yields  $V_0^\Psi = M_\beta(s_0) - M_\alpha(s_0) = \tilde{s} - \tilde{s} = 0$ .<sup>10</sup> Finally, because we have assumed that the asset prices (2.1) are driven by independent fBMs, prices are uncorrelated and thus, at time  $T$ , almost surely not identical. This implies the strict inequality  $V_T^\Psi = M_\beta(S_T) - M_\alpha(S_T) > 0$  with probability one such that arbitrage condition (iii) is also satisfied.

The result in (2.15) is the starting point for characterizing the distribution of  $V_T^\Psi$ . However, contrary to the terminal Shiryaev portfolio value covered by Proposition 2.1, closed-form distribution expressions cannot be obtained in the Salopek case. Instead, the following numerical integration method allows arbitrarily precise approximation.

**Remark 2.4 (Distribution of the terminal Salopek portfolio value)** *According to (2.15), the terminal portfolio value  $V_T^\Psi$  of the continuous-time Salopek strategy is given by  $V_T^\Psi = M_\beta(S_T) - M_\alpha(S_T)$ . From the price model (2.3) and Assumption 2.1, we deduce*

$$S_T^i = \tilde{s} \exp\{\mu^i T + \sigma^i B_T^{H^i}\} = \tilde{s} \exp\{\mu^i T + \sigma^i T^{H^i} X^i\},$$

where the  $X^i = B_T^{H^i} / T^{H^i}$ ,  $i = 1, \dots, d$ , are independent standard normal random variables. This permits writing the vector of terminal prices as  $S_T = p(X)$ , where  $X = (X^1, \dots, X^d)^\top$  is a  $d$ -dimensional standard normal random vector with the joint probability density function  $\phi_d(x) = \phi(x^1) \cdot \dots \cdot \phi(x^d)$  and  $\phi(u) = \exp\{-u^2/2\} / \sqrt{2\pi}$ . Further, the function  $p : \mathbb{R}^d \rightarrow \mathbb{R}^d$  is defined by

$$p(x) = (p^1(x^1), \dots, p^d(x^d))^\top, \quad p^i(u) = \tilde{s} \exp\{\mu^i T + \sigma^i T^{H^i} u\}, \quad i = 1, \dots, d, \quad u \in \mathbb{R}.$$

To receive the mean, variance and cumulative distribution function  $F_{V_T^\Psi}(v)$  of  $V_T^\Psi$ , we need to compute expectations of functions  $g(V_T^\Psi)$  with some  $g : \mathbb{R} \rightarrow \mathbb{R}$ . For the mean and second-order moment, we set  $g(u) = u$  and  $g(u) = u^2$ , respectively. As far as  $F_{V_T^\Psi}(v)$  is concerned, we use  $g(u) = \mathbb{1}_{\{u \leq v\}}(u)$  with indicator function  $\mathbb{1}$ . These expectations can be expressed as  $d$ -fold integrals

$$\mathbb{E}[g(V_T^\Psi)] = \int_{\mathbb{R}^d} g(M_\beta(p(x)) - M_\alpha(p(x))) \phi_d(x) dx$$

and evaluated by numerical integration. In the case of  $d = 2$  assets, which is the focus of our simulation study, we have double integrals of the form

$$\mathbb{E}[g(V_T^\Psi)] = \int_{-\infty}^{\infty} \int_{-\infty}^{\infty} g(M_\beta(p(x^1, x^2)) - M_\alpha(p(x^1, x^2))) \phi(x^1) \phi(x^2) dx^1 dx^2.$$

<sup>10</sup> Identical initial prices imply that, at time  $t = 0$ , an investor formally buys  $\hat{\Psi}_0^i(\beta) = 1/d$  shares of each asset and simultaneously sells  $\hat{\Psi}_0^i(\alpha) = 1/d$  shares of each asset.



The monotonicity property (2.13) of the  $a$ -order power mean and the portfolio value expression (2.15) suggest to choose the largest possible  $\beta$  and the smallest possible  $\alpha$ . Fusing the limits  $\beta \rightarrow \infty$  and  $\alpha \rightarrow -\infty$  into the following proposition shows that an arbitrage strategy with large  $d$  can reduce to just buying the asset  $i$  with the highest price and short-selling the asset  $j$  with the lowest price.

**Proposition 2.2** *Let  $i, j \in \{1, \dots, d\}$ ,  $t \in [0, T]$  and  $\alpha < 1 \leq \beta$  such that prices satisfy*

$$S_t^i > M_\beta(S_t) > M_\alpha(S_t) > S_t^j. \quad (2.16)$$

*Then, the strategy (2.11) has the property  $\Psi_t^i(\alpha, \beta) > 0 > \Psi_t^j(\alpha, \beta)$ . That is, the investor buys the high-priced  $i$  and short-sells the low-priced  $j$ . This particularly holds when the prices of  $i$  and  $j$  represent the maximum and minimum over all  $S_t^1, \dots, S_t^d$ .*

*Proof.* See Appendix A.3.

### 2.3 Discrete-time arbitrage

We now replace the idealized continuous-time financial market model with permanent and frictionless asset transfers by a more realistic setup where trading takes place only at a finite number of fixed points in time and is subject to transaction costs.

**Discrete-time trading.** In the discrete-time financial market model, prices are quoted at the times  $0 = t_0 < t_1 < \dots < t_N = T$ . A portfolio is created at time  $t_0 = 0$ , rebalanced at times  $t_1, \dots, t_{N-1}$  and liquidated at terminal time  $t_N = T$ . We focus on equidistant instants of time  $t_n = n\Delta t$ ,  $n = 0, \dots, N$ , which divide the total trading horizon  $[0, T]$  into  $N$  trading periods of the same length  $\Delta t = T/N$ . Thus, sampling the asset price processes (2.3) of the fractional Black-Scholes model at  $t_0, \dots, t_N$  generates a sequence of risk-free asset prices  $(S_{t_n}^0)_{n=0, \dots, N}$  and  $d$  sequences of risky asset prices  $(S_{t_n}^i)_{n=0, \dots, N}$  defined by

$$S_{t_n}^0 = 1, \quad S_{t_n}^i = s_0^i \exp \{ \mu^i t_n + \sigma^i B_{t_n}^{H^i} \}, \quad \text{for } n = 0, \dots, N \text{ and } i = 1, \dots, d,$$

with the same parameters as in Section 2.1.

It has to be expected that the discretization of a self-financing continuous-time strategy  $\Psi$ , such as the Shiryaev and Salopek strategies of Section 2.2, and the existence of transaction costs affect the self-financing property. Even without transaction costs, rebalancing a portfolio according to a discretized self-financing continuous-time strategy requires the infusion of or allows the withdrawal of capital.<sup>11</sup> These rebalancing costs and the classic transaction costs may be incorporated by modifying the risk-free asset holdings  $\Phi^0$  defined below. However, because we wish to explicitly quantify the impact of time discretization and transaction costs on continuous-time arbitrage strategies, we extend our financial market model by an additional asset  $d + 1$  which we call transaction account. In the investment fund industry, such (cash) accounts are used to react flexibly to market events (see Nascimento and Powell, 2010; Simutin, 2014). In our context, it allows us to express the aforementioned impact in monetary units. Similar to the risk-free asset price  $S^0$ , the price process of the new asset is a constant process  $S^{d+1} = (S_{t_n}^{d+1})_{n=0, \dots, N}$  with  $S_{t_n}^{d+1} = 1$ .

<sup>11</sup> In Proposition 3.1, we show that, for example, discretizing the Shiryaev strategy (2.8) almost surely leads to a strictly positive capital requirement.

We capture the trading activity of an investor by an initial capital amount  $v \in \mathbb{R}$  and the discrete-time  $\mathbb{F}$ -predictable process

$$\Phi = (\Phi_n)_{n=1, \dots, N+1} = (\Phi_n^0, \Phi_n^1, \dots, \Phi_n^{d+1})_{n=1, \dots, N+1}.$$

Here,  $\Phi_n^0$  and  $\Phi_n^{d+1} \in \mathbb{R}$  denote for  $n = 1, \dots, N$  the holdings in the risk-free asset and the transaction account, respectively, chosen at the beginning of the  $n$ -th trading period  $[t_{n-1}, t_n)$  and kept constant over that period. Further,  $\Phi_n^i \in \mathbb{R}$  is the quantity of risky asset  $i = 1, \dots, d$  held in the  $n$ -th trading period. The vector  $\Phi_{N+1}$  relates to the liquidation of the portfolio at time  $t_N = T$ . Overall,  $\Phi$  is the *discrete-time portfolio* or *trading strategy*.

Discretizing the continuous-time strategy  $\Psi = (\Psi_t)_{t \in [0, T]}$  in (2.4) leads to a piece-wise constant strategy where the investor period-wise sets and upholds  $\Psi$ . This means that, for  $i = 0, \dots, d$ , we have  $\Phi_n^i = \Psi_{t_{n-1}}^i$ ,  $n = 1, \dots, N$ , whereas liquidating the portfolio yields  $\Phi_{N+1}^i = 0$ . The positions  $\Phi_n^{d+1}$  in the transaction account are specified in what follows.

**Transaction costs.** For purchasing, rebalancing and liquidating the portfolio, the investor has to pay transaction costs depending on the *trading volume* of the risky assets. For a given strategy  $\Phi$ , at time  $t$ , this volume is defined by

$$\Gamma_t^\Phi = \begin{cases} \sum_{i=1}^d |\Phi_1^i| S_0^i, & t = t_0 = 0, & \text{(purchasing)} \\ \sum_{i=1}^d |\Phi_{n+1}^i - \Phi_n^i| S_{t_n}^i, & t = t_1, \dots, t_{N-1}, & \text{(rebalancing)} \\ \sum_{i=1}^d |\Phi_N^i| S_T^i, & t = t_N = T. & \text{(liquidating)} \end{cases} \quad (2.17)$$

We specify transaction costs proportional to the trading volume. They are determined by the proportionality factor  $p_1 \geq 0$  (in *percent*) if they exceed the minimum fee  $p_2 \geq 0$  (in *monetary units*). Otherwise,  $p_2$  is charged. We denote  $p = (p_1, p_2)$  and define the *transaction costs* for  $t = t_0, \dots, t_N$  as

$$L_t^\Phi = l(\Gamma_t^\Phi, p) \quad \text{with} \quad l(y, p) = \max(p_1 y, p_2) \mathbb{1}_{\{y > 0\}}. \quad (2.18)$$

Note that no transaction costs are charged at time  $t$  if the trading volume  $\Gamma_t^\Phi$  is zero. The special case of a model without transaction costs is reflected by  $p_1 = p_2 = 0$ .

**Liquidation.** In the continuous-time model with frictionless trading, the terminal portfolio value  $V_T^\Psi$  in (2.5) is equal to the revenue from selling the portfolio. In the discrete-time case, liquidating the portfolio induces the transaction costs  $L_{t_N}^\Phi = l(\Gamma_{t_N}^\Phi, p)$  of (2.18) and (2.17). Thus, the *net revenue* is

$$R^\Phi = \sum_{i=0}^d \Phi_N^i S_T^i - L_T^\Phi. \quad (2.19)$$

**Transaction account.** As discussed above, we have augmented our model by an asset  $d + 1$  called *transaction account*. It is used to finance rebalancing and transaction costs. Furthermore, it receives the net liquidation revenue at terminal time  $t_N = T$ . We now derive the holdings  $\Phi_n^{d+1}$ ,  $n = 1, \dots, N + 1$ , for this asset. To this end, the *rebalancing costs* of a strategy  $\Phi$  at time  $t_n$  are denoted by  $D_{t_n}^\Phi$  and defined as the value difference between the (risk-free and risky) asset holdings after and before trading:

$$\begin{aligned}
D_{t_n}^\Phi &= \sum_{i=0}^d \Phi_{n+1}^i S_{t_n}^i - \sum_{i=0}^d \Phi_n^i S_{t_n}^i = \sum_{i=0}^d (\Phi_{n+1}^i - \Phi_n^i) S_{t_n}^i \\
&= \sum_{i=0}^d (\Psi_{t_n}^i - \Psi_{t_{n-1}}^i) S_{t_n}^i, \quad n = 1, \dots, N-1.
\end{aligned} \tag{2.20}$$

Here, the last line follows from the sampling property  $\Phi_n^i = \Psi_{t_{n-1}}^i, i = 1, \dots, d$ . Also note that the rebalancing costs at time  $t_0 = 0$  and  $t_N = T$  are zero.

Aggregating the rebalancing and transaction costs as well as the net liquidation revenue, the holdings in the transaction account can be stated recursively by

$$\begin{aligned}
\Phi_1^{d+1} &= -L_0^\Phi, & (\text{purchasing}) \\
\Phi_{n+1}^{d+1} &= \Phi_n^{d+1} - D_{t_n}^\Phi - L_{t_n}^\Phi, \quad n = 1, \dots, N-1, & (\text{rebalancing}) \\
\Phi_{N+1}^{d+1} &= \Phi_N^{d+1} + R^\Phi, & (\text{liquidating})
\end{aligned} \tag{2.21}$$

where  $L_t^\Phi, R^\Phi$  and  $D_t^\Phi$  are obtained according to (2.18), (2.19) and (2.20), respectively.

**Portfolio value.** At time  $t_n$ , the value  $V_{t_n}^\Phi$  of the portfolio  $\Phi$  is

$$V_{t_n}^\Phi = \sum_{i=0}^{d+1} \Phi_{n+1}^i S_{t_n}^i, \quad n = 0, \dots, N. \tag{2.22}$$

$V^\Phi = (V_{t_n}^\Phi)_{n=0, \dots, N}$  is the *discrete-time value process*. While, at time  $t = 0$ , the continuous-time model yields  $V_{t_0}^\Psi = v$ , the discrete-time case delivers  $V_0^\Phi = v - L_0^\Phi$ . That is, the portfolio value equals the initial capital minus the transaction costs for purchasing the portfolio. If  $\Phi$  results from discretizing a continuous-time arbitrage strategy  $\Psi$  with  $V_0^\Psi = v = 0$ , the discrete-time value process starts with  $V_0^\Phi = -L_0^\Phi \leq 0$ . This term is strictly negative if the initial trading volume  $\Gamma_0^\Phi$  and at least one of the two transaction cost parameters  $p_1$  and  $p_2$  are positive. For the terminal trading time  $t_N = T$ , substituting  $\Phi_{N+1}^0 = \dots = \Phi_{N+1}^d = 0$  into (2.22) and applying (2.21) provides  $V_T^\Phi = \Phi_{N+1}^{d+1} S_{t_N}^{d+1} = \Phi_N^{d+1} + R^\Phi$ . Hence, the terminal portfolio value equals the net liquidation revenue  $R^\Phi$  minus the cumulated rebalancing and transaction costs  $\Phi_N^{d+1}$  for trading at times  $t_0, \dots, t_{N-1}$ .

**Remark 2.5** For a continuous-time arbitrage strategy  $\Psi$ , we know from Remark 2.1 that scaling the strategy by some factor  $\gamma > 0$  preserves the arbitrage property.  $\tilde{\Psi} = \gamma\Psi$  is also an arbitrage strategy. For the value process, we have  $V^{\gamma\Psi} = \gamma V^\Psi$ . A time discretization of  $\Psi$  and transaction costs generally destroy the arbitrage property. However, inspecting the construction of the discretized strategy  $\Phi$  reveals that we preserve the scaling property of the discrete-time value process  $V^{\gamma\Phi} = \gamma V^\Phi$  as long as the transaction costs are defined with a floor  $p_2 = 0$ , i.e., only proportional transaction costs  $L_t^\Phi = p_1 \Gamma_t^\Phi$  are charged.

Finally, it is noteworthy that the discrete-time value process  $V^\Phi$  satisfies a generalized self-financing condition

$$V_{t_n}^\Phi - L_{t_n}^\Phi = V_{t_n}^\Phi, \quad n = 0, \dots, N-1,$$

where  $V_{t_n}^\Phi = \sum_{i=0}^{d+1} \Phi_n^i S_{t_n}^i$  is the portfolio value before rebalancing at  $t_n, n = 1, \dots, N-1$ , and  $V_{0-}^\Phi = v$ . This condition formalizes the property that the value after rebalancing equals the value before rebalancing minus the transaction costs of the corresponding trade.

**Portfolio value differences.** The continuous and discrete portfolio values (2.5) and (2.22), respectively,  $\Phi_n^i = \Psi_{t_{n-1}}^i$ ,  $n = 1, \dots, N$ , and  $S_t^{d+1} = 1$  allow us to express the performance of the discretized strategy  $\Phi$  relative to  $\Psi$  in terms of transaction account holdings:

$$V_t^\Phi - V_t^\Psi = \Phi_t^{d+1} \quad \text{for } t = t_0, \dots, t_{N-1}. \quad (2.23)$$

While (2.23) only holds before liquidation, the following lemma presents a more general relationship for all times  $t$ , i.e., including the liquidation date  $t = t_N = T$ .

**Lemma 2.1** *For  $t = t_0, \dots, t_N$ , the difference between the portfolio values  $V_t^\Psi$  and  $V_t^\Phi$  can be formulated as*

$$V_t^\Psi - V_t^\Phi = \mathcal{D}_t + \mathcal{L}_t, \quad \text{with } \mathcal{D}_t = \sum_{t_n \leq t} D_{t_n}^\Phi \quad \text{and} \quad \mathcal{L}_t = \sum_{t_n \leq t} L_{t_n}^\Phi, \quad (2.24)$$

where the summation terms  $\mathcal{D}_t$  and  $\mathcal{L}_t$  denote the cumulated rebalancing and transaction costs in the period  $[0, t]$ , respectively.

*Proof.* See Appendix A.2.

In a situation without transaction costs, the decomposition in Lemma 2.1 implies that the loss in terminal portfolio value, i.e., the *discretization error*, going along with the discrete-time transfer of the continuous-time strategy  $\Psi$  is

$$\mathcal{D}_T = V_T^\Psi - V_T^\Phi. \quad (2.25)$$

In Propositions 3.2 and 3.3 below, we study the asymptotic behavior of this quantity for an increasing trading frequency, i.e., for  $N \rightarrow \infty$  such that  $\Delta t \rightarrow 0$ .

### 3 Simulation study

#### 3.1 Parameters and data generation

To provide a full-scale analysis of our two arbitrage strategies, we conduct a Monte Carlo study and a complementary mathematical analysis of discretization error based on the model and trading parameters of Table 3.1. This table captures our *basis setting* which will be successively modified and relaxed as we proceed.

Guided by the empirical literature (see Willinger et al., 1999; Bessembinder, 2018), we start by specifying suitable drifts  $\mu^i$ , volatilities  $\sigma^i$  and Hurst parameters  $H^i$  for the  $d$  risky assets of the Shiryayev and Salopek strategies. We restrict the latter to  $d = 2$  assets and assume that they have identical parameters. We also set the initial prices to  $\tilde{s} = 100$ .

We then consider an investor with a  $T = 1$  year investment horizon subdivided into  $N = 250$  trading days (see Hendricks and Singhal, 2005). This investor is assumed to follow the discretization of Section 2.3 to trade the strategies of Section 2.2 at a daily frequency. All transaction costs  $p$  are zero. To capture the performance of this investor, we simulate 100,000 asset price scenarios and scenario-wise document  $V_T^\Phi$ , i.e., the portfolio value after liquidation.<sup>12</sup> Consequently, for each strategy (and parameter setting), our Monte Carlo study delivers a distribution of  $V_T^\Phi$  values which will undergo detailed analysis.

<sup>12</sup> This number of simulation repetitions ensures stable results (see Schuhmacher and Eling, 2011).

Risky assets	Number of assets	$d$	1 (Shiryaev), 2 (Salopek)
	Drift	$\mu^i$	0.05
	Volatility	$\sigma^i$	0.1
	Hurst coefficient	$H^i$	0.6
	Initial value	$s_0^i = \tilde{s}$	100
Trading	Trading horizon	$T$	1
	Trading periods	$N$	250
	Trading dates	$t_n$	$n\Delta t = n/N, \quad n = 0, \dots, N$
	Transaction costs	$p = (p_1, p_2)$	(0, 0)
	Scaling factor	$\gamma$	100
	Salopek specification	$(\alpha, \beta)$	(-30, 30)

This table summarizes the model parameters of the risky assets  $i = 1, 2$  (see Sections 2.1 and 2.2) and the discrete-time trading parameters (see Sections 2.2 and 2.3) we use in our simulation basis setting.

Table 3.1: Basis setting

To generate a path of a discrete-time fBm many algorithms have been proposed in the literature (see Kijima and Tam, 2013). They can be grouped into exact and approximate methods. While the first category fully preserves the key properties of a fBm at the cost of higher computation time, the second group sacrifices some accuracy to improve time efficiency. Practitioners are often interested in quick results and therefore tend to favor spectral simulation techniques of the approximate class (see Dieker and Mandjes, 2003). We opt for an exact approach, i.e., the circulant embedding method of Wood and Chan (1994), because we wish to rule out any influence of approximation error on our evaluation of strategy performance.<sup>13</sup> This method competes quite well with the speed of approximate methods (see Coeurjolly, 2000) and, given the fact that simulation source code is readily available, its implementation is straightforward (see Kroese and Botev, 2015).<sup>14</sup>

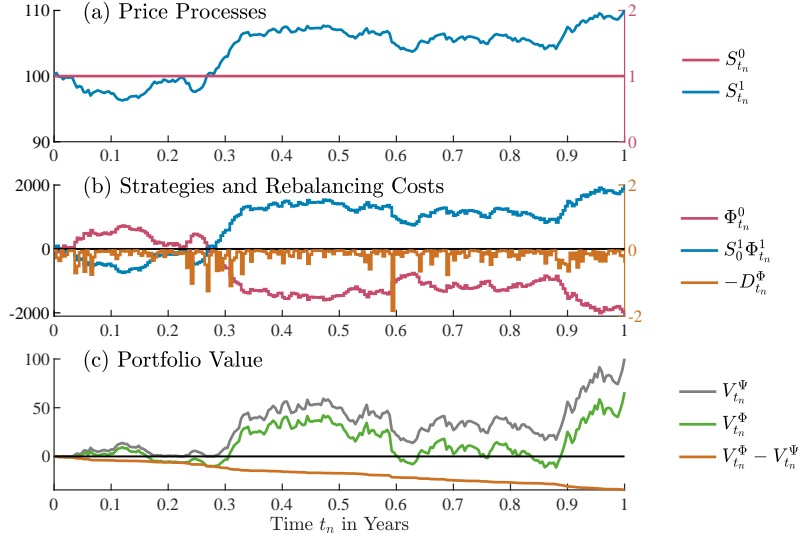
## 3.2 Discretized Shiryaev strategy

### 3.2.1 General strategy behavior

We start with the Shiryaev strategy which trades the risk-free asset and one risky asset. For this strategy and our basis setting of Table 3.1, Figure 3.1 presents a typical realization of our simulations. Panel (a) plots the daily prices  $S_{t_n}^0 = 1$  and  $S_{t_n}^1$  of the risk-free and the risky asset, respectively. Panel (b) describes the daily strategy  $\Phi$  and the associated rebalancing costs  $D_{t_n}^\Phi$ . For visual convenience, we scale the number of risky assets by the initial risky asset price  $S_0^1 = \tilde{s}$  and show the *negative* costs  $-D_{t_n}^\Phi$ . Because of  $p = (0, 0)$  and (2.21), the holdings  $\Phi_n^2$  in the transaction account result from cumulating the rebalancing costs, i.e.,  $\Phi_1^2 = 0, \Phi_{n+1}^2 = \Phi_n^2 - D_{t_n}^\Phi, n = 1, \dots, N - 1$ . Finally, Panel (c) illustrates the value process  $V^\Psi$  of the continuous-time strategy  $\Psi$ , the value process  $V^\Phi$  of the discretized strategy  $\Phi$

<sup>13</sup> Independent of Wood and Chan (1994), the study of Dietrich and Newsam (1997) has developed the same simulation technique. Stein (2002) discusses non-stationary surface extensions. In an earlier draft, we used the closely related approximate method of Yin (1996). It delivered slightly different performance metrics but allowed the same overall conclusions.

<sup>14</sup> We follow the starting value recommendation of Danuirdjo and Hirose (2011). Due to the Fourier transform nature of the method, a single simulation run always generates two independent fBm realizations (see Dietrich and Newsam, 1997).



For the discretized Shiryayev strategy and our basis setting of Table 3.1, this figure plots a typical simulation result. Panel (a) shows the realized prices  $S_{t_n}^0$  and  $S_{t_n}^1$  of the risk-free and the risky asset, respectively. Panel (b) illustrates the strategy holdings  $\Phi_{t_n}^0$  and  $\Phi_{t_n}^1$  for these assets where the latter has been multiplied by  $S_0^1$ . Furthermore, it contains the negative rebalancing costs  $-D_{t_n}^\Phi$ . Finally, Panel (c) reports the portfolio value  $V_{t_n}^\Phi$  of the strategy. It is supplemented by the value process  $V_{t_n}^\Psi$  of continuous-time trading and the difference between both portfolio values which, except for terminal time  $t_N = T = 1$ , is equal to the holdings  $\Phi_{t_n}^2$  in the transaction account.

Fig. 3.1: Exemplary realization of the discretized Shiryayev strategy

and the difference between them. As shown in (2.23), this difference equals the holdings  $\Phi_{t_n}^2$  in the transaction account for  $t_n = t_0, \dots, t_{N-1}$ .

According to (2.8), a Shiryayev-type investor enters a long (short) position in the risky asset whenever the risky asset price exceeds (falls below) the initial risky asset price. The opposite applies to the risk-free asset. This can be seen in Panels (a) and (b). We also observe that the rebalancing costs  $D_{t_n}^\Phi$  are small and always positive; this is validated in Proposition 3.1. Thus, each rebalancing activity requires new capital and increases the absolute value of the negative holdings  $\Phi^2$  in the transaction account. In Panel (c), this leads to a growing difference between the portfolio values of continuous and discrete trading.

**Proposition 3.1** *For the rebalancing costs (2.20) of the discretized Shiryayev strategy (2.8) and  $n = 1, \dots, N - 1$ , it holds almost surely that*

$$D_{t_n}^\Phi = \frac{(S_{t_n}^1 - S_{t_{n-1}}^1)^2}{s_0^1} > 0. \quad (3.1)$$

*Proof.* See Appendix A.4.

We know from (2.9) that the portfolio value of the continuous-time arbitrage strategy is  $V_t^\Psi = (S_t^1 - s_0^1)^2 / s_0^1 \geq 0$ . It rises with the distance between the risky asset price  $S_t^1$  and the initial risky asset price  $s_0^1$ . In other words, the strategy benefits from prices rising above  $s_0^1$  and from prices falling below  $s_0^1$ . As indicated in Remarks 2.1 and 2.5, scaling the continuous-time strategy  $\Psi$  by some factor  $\gamma > 0$  preserves the arbitrage property and leads to a scaling of the value processes  $V^\Psi$  and  $V^\Phi$  by the same factor. Looking at the terminal value  $V_T^\Phi \approx 65$ , we can deduce that raising the basis scaling factor of  $\gamma = 10^2$  to say  $\gamma = 10^5$  increases the terminal value to roughly 65,000. Hence, the absolute size of the portfolio value is not relevant for evaluating the performance of the strategy.

### 3.2.2 Impact of time discretization and transaction costs

After examining a single simulation scenario in the parameter basis setting, we now turn to the results of 100,000 scenarios and additionally introduce transaction costs.

Panel (a) of Figure 3.2 visualizes the simulated distribution of the terminal portfolio value  $V_T^\Psi$  for continuous-time trading and the corresponding  $V_T^\Phi$  distributions for the discrete-time case with three different transaction cost variants.  $p = (0, 0)$  resembles no transaction costs.  $p = (0.1, 0)$  considers only proportional costs, whereas  $p = (0.1, 0.5)$  additionally includes a minimum fee. Recall that the proportional values are expressed in percent. The chosen cost magnitudes are guided by what are currently very low commissions and brokerage fees (see Auer and Schuhmacher, 2015). Table 3.2 provides summary statistics for the distributions and concisely evaluates the performance of the trading strategy. Here, we are particularly interested in the mean terminal value and the loss probability because they capture  $\mathbb{E}[V_T^\Phi]$  and  $\mathbb{P}(V_T^\Phi < 0)$ , respectively.

We observe that the Shiryaev strategy  $\Psi$  is an arbitrage strategy with positive terminal values  $V_T^\Psi$  in all scenarios. The distribution of  $V_T^\Psi$  is characterized by positive skewness, a wide right tail and a mean of 144.7. This simulated value is very close to its theoretical counterpart of 144.2 which can be obtained via Proposition 2.1.<sup>15</sup> In comparison, discretizing the strategy yields a terminal value  $V_T^\Phi$  distribution of similar shape but shifted towards smaller values and partially into negative territory. Without transaction costs, the range of observed terminal values is  $[-53.5; 4,392.8]$ . This means that the maximum gain is significantly higher than the maximum loss. With a value of 109.4, the mean of  $V_T^\Phi$  is more than double the maximum loss, covers about 75% of the mean of  $V_T^\Psi$  and can be earned by accepting a loss probability of only 39%.

Proposition 3.2 presents an asymptotic expansion of the expected cumulated Shiryaev rebalancing costs  $\mathcal{D}_T$  (with zero transaction costs) for an increasing trading frequency, i.e.,  $N \rightarrow \infty$  such that  $\Delta t \rightarrow 0$ . Because (2.25) implies  $V_T^\Phi = V_T^\Psi - \mathcal{D}_T$ , it can be used to formally proxy  $\mathbb{E}[V_T^\Phi]$  instead of depicting it via simulation. Specifically, the leading term  $C\Delta t^{2H-1}$  of the expansion, where  $C$  and  $2H - 1$  are the rate and order of convergence, respectively, delivers the approximation 109.0 and proves to be quite accurate (see also Tables 3.3 to 3.5 and, in particular, Table 3.6).<sup>16</sup>

**Proposition 3.2 (Expected cumulated Shiryaev rebalancing costs)** *For a discretization with step size  $\Delta t = T/N$ ,  $N \in \mathbb{N}$ , and  $\Delta t \rightarrow 0$ , the expectation of the cumulated rebalancing costs of the Shiryaev strategy  $\mathcal{D}_T = \mathcal{D}_T(\Delta t) = \sum_{n=1}^N D_n^\Phi$  given in (2.24) satisfies*

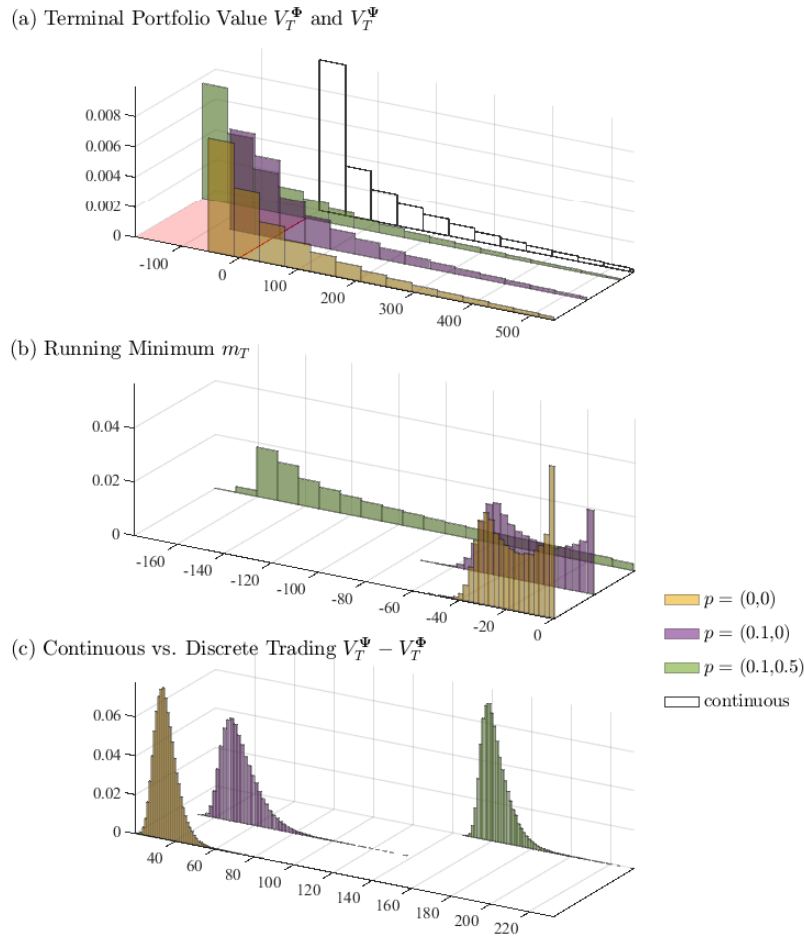
$$\mathbb{E}[\mathcal{D}_T(\Delta t)] = C\Delta t^{2H-1} + o(\Delta t^{2H-1}) \quad \text{with} \quad C = \sigma^2 s_0^1 \int_0^T \exp\{2\mu t + 2\sigma^2 t^{2H}\} dt.$$

*Proof.* See Appendix A.5.

In line with intuition, transaction costs shift the portfolio value distribution even further such that losses become higher and more likely. For  $p = (0.1, 0)$ , the mean of  $V_T^\Phi$  falls to

<sup>15</sup> The asymptotic  $(1 - \alpha)$  confidence interval for the mean  $m$  is  $\hat{m} \pm \frac{\hat{s}}{\sqrt{n}} z_{1-\alpha/2}$ . For an empirical mean and standard deviation of  $\hat{m} = 144.7$  and  $\hat{s} = 226.2$ , respectively, a sample size of  $n = 100,000$ , and  $\alpha = 5\%$ , we have  $(143.3, 146.1)$ . The theoretical value of  $m = 144.2$  is covered by this range.

<sup>16</sup> We recognize the order  $2H - 1$  from the convergence to zero of the fBm's quadratic variation restricted to the time grid (see Lin, 1995). The quality statement can be backed up similar to Footnote 15.



For 100,000 simulated scenarios of the discretized Shiryayev strategy, the basis setting of Table 3.1 and a range of transaction cost values, this figure presents various portfolio value distributions. Panel (a) shows the distributions of the terminal value  $V_T^\Phi$  of discrete-time trading with transaction costs  $p = (p_1, p_2)$  where  $p_1$  reflects proportional costs (in percent) and  $p_2$  is a minimum fee (in monetary units). The loss region with negative terminal values is highlighted by a red floor. The distribution of the terminal value  $V_T^\Psi$  of continuous-time trading is also included. Panel (b) contains the distributions of the running minimum  $m_T$  of the discrete value processes, i.e., the worst-case portfolio values in the investment horizon. Finally, the distributions in Panel (c) refer to the terminal difference  $V_T^\Psi - V_T^\Phi$  between continuous-time and discrete-time trading. For better visibility, the x-axis in Panel (a) is cut off after the 95% quantile of  $p = (0,0)$ .

Fig. 3.2: Shiryayev portfolio value distributions for different transaction costs

Strat.	Transact. costs $p$	Mean	Stand. dev.	Min	Quantiles				Loss prob.
					5%	Median	95%	Max	
$\Psi$	none	144.7 (144.2)	226.2 (222.9)	0.0 (0.0)	0.5 (0.5)	59.4 (59.6)	581.3 (575.7)	4,477.2 ( $\infty$ )	0.00 (0.00)
$\Phi$	(0,0)	109.4	222.8	-53.5	-32.9	25.7	537.9	4,392.8	0.39
	(0.1,0)	91.9	219.7	-73.7	-48.1	9.2	514.2	4,339.9	0.46
	(0.1,0.5)	-17.3	221.0	-178.5	-157.9	-100.4	407.8	4,245.5	0.73

This table reports some descriptive statistics for the simulated terminal portfolio value distributions in Panel (a) of Figure 3.2. Besides the mean and standard deviation, we compute the minima and maxima as well as selected quantiles. Furthermore, we present the simulated loss probability, i.e., the proportion of negative terminal portfolio values. The numbers in parentheses for the continuous-time portfolio represent theoretical values obtained via Proposition 2.1.

Table 3.2: Shiryayev portfolio value statistics for different transaction costs

91.9 but remains positive. Simultaneously, the loss probability rises to 46% but can still



be considered reasonably low (see Hogan et al., 2004). In contrast,  $p = (0.1, 0.5)$  generates a negative mean of  $-17.3$  and a loss probability of 73%. The reason for this drastic impact of the minimum fee is that our basis setting is of low monetary scale such that the daily trading volumes are small and the minimum fee applies frequently. For  $N = 250$  trades, this often results in a total fee of  $250 \times p_2 = 125$  offsetting gains and causing high losses. Overall, while proportional transaction costs only slightly reduce the performance of the discretized strategy, minimum fees can render it unattractive for small-scale investors. However, medium-scale investors with a higher scaling factor  $\gamma$  and thus higher trading volumes do not suffer from this kind of problem.<sup>17</sup>

Panel (b) of Figure 3.2 conducts a worst-case analysis similar to drawdown calculations in active risk management (see Schuhmacher and Eling, 2011). For  $t \in [0, T]$ , we define the running minimum process associated with the discrete-time value process  $V^\Phi$  as

$$m_t := \min_{t_n \leq t} V_{t_n}^\Phi.$$

With  $t = T$ , we obtain  $m_T$  representing the least favorable portfolio value in the investment horizon  $[0, T]$ . The simulated distributions of  $m_T$  show that its upper bound is zero because, across our transaction cost variants, we have  $V_0^\Phi \leq 0$ . The smallest values of  $m_T$  are close to the minima of the terminal values  $V_T^\Phi$  in Panel (a). However, a frequency comparison reveals that the vast majority of worst-case events do not cluster at time  $T$ .

Finally, Panel (c) shows the simulated distributions of the difference  $V_T^\Psi - V_T^\Phi$  between the terminal portfolio values of continuous-time trading and its discrete-time counterparts. Discrepancies obviously rise with  $p$ . More demanding transaction cost variants require higher capital infusions, i.e., a more intensive usage of the transaction account.

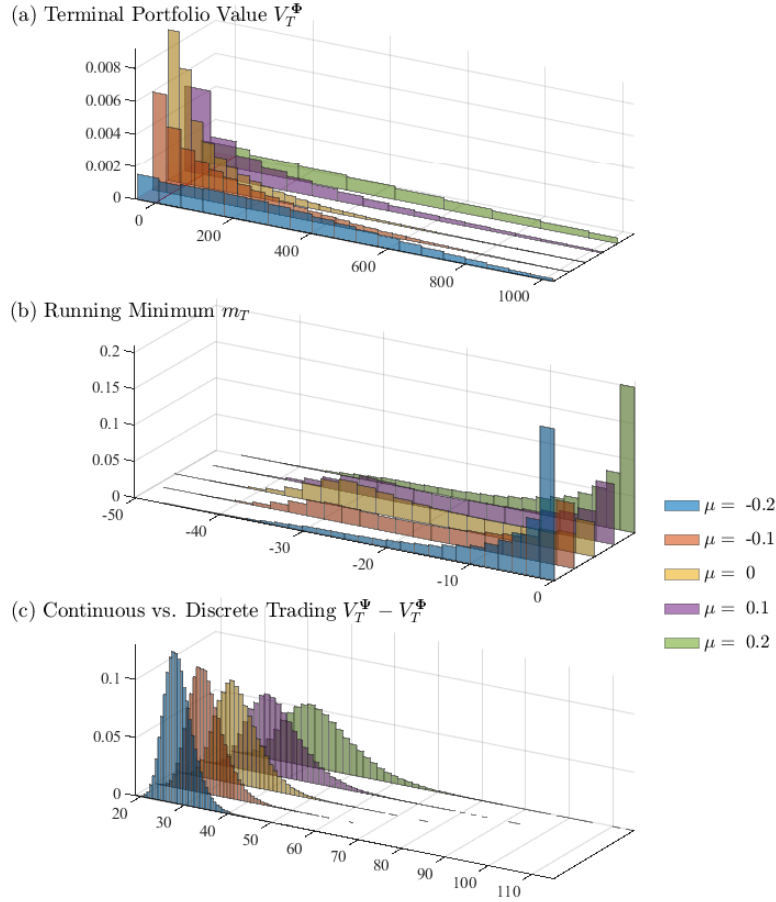
### 3.2.3 Impact of asset model parameters

To implement the Shiryaev strategy, investors have to select a suitable risky asset. To support this choice, we study the impact of the asset parameters  $(\mu, \sigma, H)$  on the performance of the strategy. This primarily involves constructing figures and tables in the style of Figure 3.2 and Table 3.2. However, instead of  $p$ , we now vary  $(\mu, \sigma, H)$ .

**Drift  $\mu$ .** Figure 3.3 and Table 3.3 start by considering the alternative drift parameters  $\mu \in \{0, \pm 0.1, \pm 0.2\}$ . Assets with higher absolute mean returns  $\mu$  shift, flatten and extend the distribution of  $V_T^\Phi$  towards larger terminal values because, *ceteris paribus*, they fuel the strategy with more extreme prices. This effect is stronger for positive than for negative  $\mu$  because upward movements are unbounded, whereas downward movements have a floor at a price level of zero.<sup>18</sup> For example, starting from 69.2 for  $\mu = 0$ , the mean terminal value is 209.1 for  $\mu = 0.1$  but only 136.1 for  $\mu = -0.1$ . In contrast, the loss probabilities are quite symmetric in  $\mu$ . From 43% for  $\mu = 0$ , they fall to about 28% for  $|\mu| = 0.1$  and to 7% for  $|\mu| = 0.2$ . A similar feature can be observed for the running minimum  $m_T$ . For  $\mu = 0$ , its distribution is almost uniform. For rising  $|\mu|$ , peaks near zero become more pronounced and excursions of the portfolio value significantly below zero less likely.  $V_T^\Psi - V_T^\Phi$  is not symmetric in  $\mu$ . Instead, the distribution support increases with  $\mu$  towards larger values. Hence, a higher  $\mu$  induces more rebalancing costs in discrete-time trading.

<sup>17</sup> In contrast to large-scale traders, medium-scale traders are often considered to have insignificant market impact (see Bouchaud, 2022).

<sup>18</sup> A similar rationale explains differences in the prices of at-the-money call and put options with identical underlying, strike and maturity (see Black and Scholes, 1973).



Similar to the Shiryayev strategy Figure 3.2, but for varying drift values  $\mu$ , this figure presents the simulated distributions of (a) the terminal portfolio value  $V_T^\Phi$ , (b) the running value process minimum  $m_T$  and (c) the difference  $V_T^\Psi - V_T^\Phi$  between the terminal portfolio values of continuous-time and discrete-time trading. For better visibility, the x-axis in Panel (a) ends at the 80% quantile of  $\mu = 0.2$ .

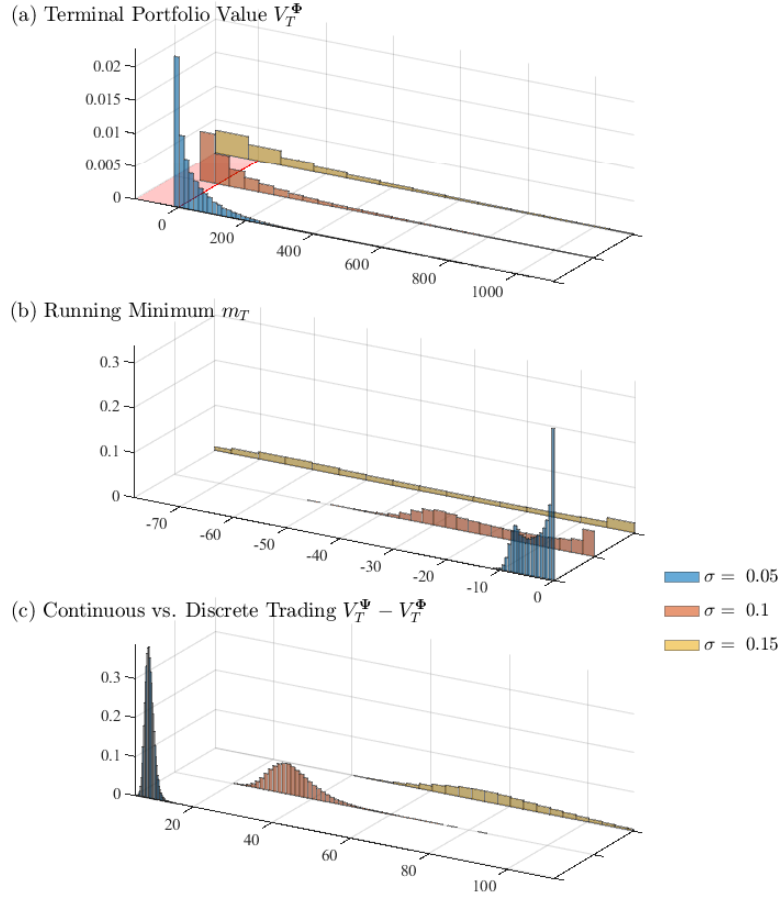
Fig. 3.3: Shiryayev portfolio value distributions for different drifts

$\mu$	Mean	Median	Stand. dev.	Min	Max	Loss prob.
-0.2	355.0 (354.4)	301.5	291.6	-46.5	2,098.7	0.07
-0.1	136.1 (134.9)	71.5	187.4	-48.2	1,842.4	0.27
0.0	69.2 (68.3)	12.8	153.2	-50.1	3,377.4	0.43
0.1	209.1 (209.5)	82.7	334.4	-47.6	5,602.4	0.28
0.2	625.0 (628.0)	446.1	641.8	-46.7	8,706.9	0.07

Similar to Table 3.2, this table reports some descriptive statistics for the simulated terminal portfolio value distributions in Panel (a) of Figure 3.3. The mean values in parentheses are approximations based on Proposition 3.2.

Table 3.3: Shiryayev portfolio value statistics for different drifts

**Volatility  $\sigma$ .** Figure 3.4 and Table 3.4 present our sensitivity results for the volatilities  $\sigma \in \{0.05, 0.10, 0.15\}$ . Increasing volatility goes along with a greater variability of terminal portfolio values  $V_T^\Phi$ . Large gains and large losses become more likely. This is also evident in the stretching distributions of the running minimum  $m_T$ . The mean terminal values increase with  $\sigma$  and so do the loss probabilities. For example,  $\sigma = 0.05$  delivers 46.6 and 27%, whereas  $\sigma = 0.15$  yields 218.5 and 41%. Thus, if investors are prepared to bear



Similar to the Shiryayev strategy Figure 3.2, but for varying volatility values  $\sigma$ , this figure presents the simulated distributions of (a) the terminal portfolio value  $V_T^\Phi$ , (b) the running value process minimum  $m_T$  and (c) the difference  $V_T^\Psi - V_T^\Phi$  between the terminal portfolio values of continuous-time and discrete-time trading. For better visibility, the x-axis in Panels (a) and (c) (Panel (b)) ends at the 95% quantile (starts at the 5% quantile) of  $\sigma = 0.15$ .

Fig. 3.4: Shiryayev portfolio value distributions for different volatilities

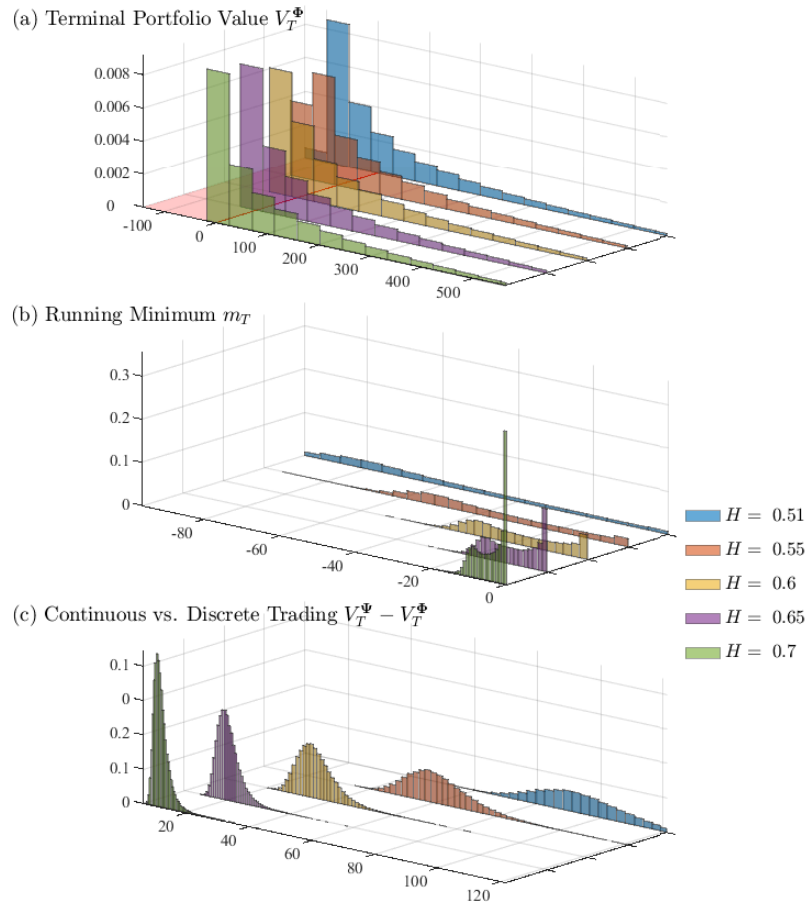
$\sigma$	Mean	Median	Stand. dev.	Min	Max	Loss prob.
0.05	46.6 (46.7)	19.9	71.4	-11.3	1,036.6	0.27
0.10	109.4 (109.0)	25.7	222.8	-53.5	4,392.8	0.39
0.15	218.5 (217.0)	41.1	494.9	-125.6	11,927.1	0.41

Similar to Table 3.2, this table reports some descriptive statistics for the simulated terminal portfolio value distributions in Panel (a) of Figure 3.4. The mean values in parentheses are approximations based on Proposition 3.2.

Table 3.4: Shiryayev portfolio value statistics for different volatilities

more risk in exchange for higher reward, they have an incentive to opt for volatile assets (see Frazzini and Pedersen, 2014). However, it must be noted that the rebalancing costs of discrete trading, which are resembled by  $V_T^\Psi - V_T^\Phi$ , substantially increase with  $\sigma$ .

**Hurst parameter  $H$ .** In Figure 3.5 and Table 3.5, we investigate the Hurst coefficients  $H \in \{0.51, 0.55, 0.60, 0.65, 0.70\}$ . Recall that  $H = 0.5$  implies no memory and elevating  $H$  within the interval  $(0.5, 1)$  establishes long memory. It generates positive serial correlation



Similar to the Shiryaeve strategy Figure 3.2, but for varying Hurst coefficients  $H$ , this figure presents the simulated distributions of (a) the terminal portfolio value  $V_T^\Phi$ , (b) the running value process minimum  $m_T$  and (c) the difference  $V_T^\Psi - V_T^\Phi$  between the terminal portfolio values of continuous-time and discrete-time trading. For better visibility, the x-axis in Panels (a) and (c) (Panel (b)) ends at the 95% quantile of  $H = 0.7$  and  $H = 0.51$ , respectively (starts at the 5% quantile of  $H = 0.51$ ).

Fig. 3.5: Shiryaeve portfolio value distributions for different Hurst coefficients

$H$	Mean	Median	Stand. dev.	Min	Max	Loss prob.
0.51	49.6 (49.0)	-31.7	218.9	-141.5	3,787.8	0.60
0.55	83.5 (83.0)	0.7	221.1	-91.7	4,084.4	0.50
0.60	109.4 (109.0)	25.7	222.8	-53.5	4,392.8	0.39
0.65	124.2 (123.9)	40.0	223.7	-31.4	4,640.3	0.30
0.70	132.7 (132.5)	48.3	224.1	-18.4	4,831.5	0.23

Similar to Table 3.2, this table reports some descriptive statistics for the simulated terminal portfolio value distributions in Panel (a) of Figure 3.5. The mean values in parentheses are approximations based on Proposition 3.2.

Table 3.5: Shiryaeve portfolio value statistics for different Hurst coefficients

with levels linked to  $H$  and high even for distant lags. Shiryaeve-type investors take long (short) positions in the risky asset when its price deviates from an initial state in positive (negative) direction. Thus, they can benefit directly from a trending behavior of the risky asset which is more likely under high than low  $H \in (0.5, 1)$ . Specifically, with rising  $H$ , the distributions of  $V_T^\Phi$  and  $m_T$  relocate and reform such that the likelihood of large gains

(losses) increases (decreases). Switching from  $H = 0.6$  to  $H = 0.7$ , for example, raises the mean terminal value from 109.4 to 132.7 and lowers the loss probability from 39% to 23%. Interestingly, this is accompanied by a sharp drop in rebalancing costs  $V_T^\Psi - V_T^\Phi$ . Hence, investors should trade assets with high  $H$ , which have been identified in many asset classes (see Hiemstra and Jones, 1997; Auer, 2016; Coakley et al., 2016), because they make the strategy more secure and less cash-intensive with respect to the transaction account.

### 3.2.4 Impact of trading horizon and frequency

Besides a suitable risky asset, Shiryayev-type investors have to decide on the trading horizon and frequency. Thus, it is instructive to know how they affect portfolio performance.

**Trading horizon.** In a first experiment, we fix the trading frequency to daily and vary the trading horizon  $T$  between 6 months and 10 years. As far as the remaining parameters are concerned, we use the basis setting of Table 3.1 and the additional transaction cost settings of Figure 3.2 and Table 3.2. For each setting and trading horizon, we simulate 100,000 scenarios and report the mean terminal portfolio value and the loss probability in Figure 3.6. Panel (a) illustrates that the mean increases with the trading horizon and, except for the shortest horizons and the highest transaction costs, is positive-valued. Relation (2.10) tells us that, for large  $T$ , the expected terminal wealth  $\mathbb{E}[V_T^\Psi]$  of the continuous-time Shiryayev strategy grows just like  $s_0^1 \exp\{2\mu T + 2\sigma^2 T^{2H}\}$ . This exceeds exponential growth in  $T$  because  $H > 0.5$ . A similar behavior can be observed for the discretized strategy. Panel (b) shows that the loss probabilities initially notably decrease with  $T$  and then tend to stabilize. The marginal reduction becomes less pronounced and, under proportional costs, we even reach probabilities close to 20%. The differences between transaction cost variants also shrink with  $T$  and stabilize. This can be explained by successively rising daily trading volumes eliminating minimum fee dominance.

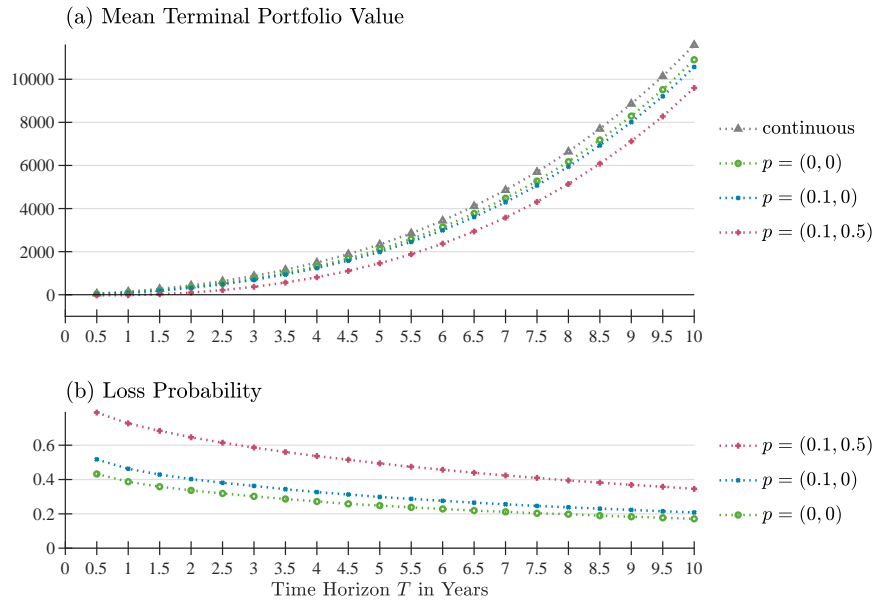
**Trading frequency.** In a reverse second experiment, we fix the trading horizon to  $T = 1$  year and vary the trading frequency. We evaluate monthly, two-weekly, weekly, two-daily and daily rebalancing corresponding to  $N \in \{12, 25, 50, 125, 250\}$  trading periods per year.<sup>19</sup> Figure 3.7 presents the simulation outcomes for our three transaction cost settings, i.e., the mean terminal value and the loss probability as functions of the trading frequency. The results for trading without transaction costs and only proportional costs are similar. The mean terminal value increases with the trading frequency but there is still a clear difference to continuous-time trading.<sup>20</sup> The loss probability decreases with the trading frequency.<sup>21</sup> For investors facing a supplementary minimum fee, the mean terminal value sharply drops with the trading frequency and reaches a negative value for daily trading. At the same time, the loss probability rises to more than 70%. This feature is again caused by the scale-related relative size of proportional costs and the minimum fee.

Besides supplying investment-relevant insights, simulations with rising  $N$  allow us to verify the approximation quality and the convergence speed of the rebalancing cost expression derived in Proposition 3.2. For several trading frequencies, Table 3.6 compares

<sup>19</sup> We do not consider frequencies higher than daily because, in this context, our assumption of independent asset prices would no longer be realistic (see Malceniace et al., 2019).

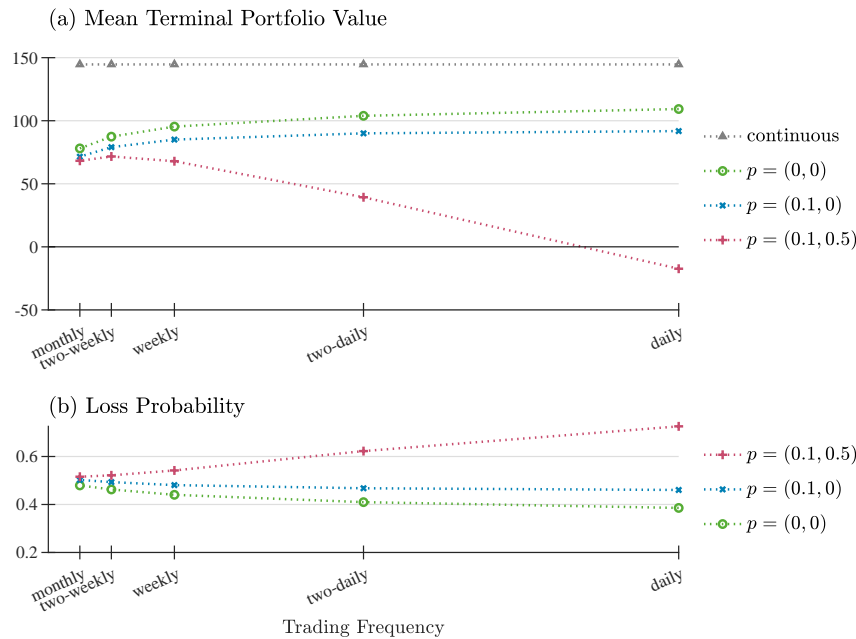
<sup>20</sup> For  $p = (0, 0)$ , the difference disappears when the trading frequency tends to infinity.

<sup>21</sup> For  $p = (0, 0)$ , the limiting probability is zero.



For 100,000 simulated scenarios of the discretized Shiryayev strategy, the basis setting of Table 3.1 and a range of transaction cost values  $p$ , this figure plots (a) the mean of the terminal portfolio value and (b) the simulated loss probability against the trading horizon  $T$ . The continuous case is included as a reference.

Fig. 3.6: Shiryayev sensitivity to trading horizon



For 100,000 simulated scenarios of the discretized Shiryayev strategy, the basis setting of Table 3.1 and a range of transaction cost values  $p$ , this figure plots (a) the mean of the terminal portfolio value and (b) the simulated loss probability against the trading frequency. The continuous case is included as a reference.

Fig. 3.7: Shiryayev sensitivity to trading frequency

the simulated  $\mathbb{E}[V_T^\Phi]$  with the approximated  $\mathbb{E}[V_T^\Phi]$ . We observe that they are very close to each other. Interestingly, this even holds for the lowest considered trading frequency,

Frequency	$N$	$\mathbb{E}[V_T^\Phi]$		$(\mathbb{E}[V_T^\Psi - V_T^\Phi]) / \Delta t^{2H-1}$
		simulated	approximated	simulated
Monthly	12	77.1	79.6	109.6
Two-weekly	25	87.4	88.4	109.2
Weekly	50	95.3	95.6	108.0
Two-daily	125	103.9	103.4	107.2
Daily	250	109.4	109.0	106.6
	$\infty$	144.7	$\mathbb{E}[V_T^\Psi] = 144.2$	$C = 106.2$

For several trading frequencies of the Shiryaev strategy and the basis setting of Table 3.1, this table contrasts the simulated and the approximated values of  $\mathbb{E}[V_T^\Phi]$  where the latter are obtained via Proposition 3.2. The numbers in the last line represent the simulated and exact values of  $\mathbb{E}[V_T^\Psi]$  taken from Table 3.2. The last table column divides the simulated value of  $\mathbb{E}[V_T^\Psi - V_T^\Phi]$  by  $\Delta t^{2H-1}$ .  $C$  is the rate of convergence in Proposition 3.2.

Table 3.6: Shiryaev mean approximation

i.e., monthly rebalancing with only  $N = 12$  trades, where the deviation amounts to just about 3%. Furthermore, noting that  $\mathbb{E}[\mathcal{D}_T(\Delta t)] = \mathbb{E}[V_T^\Psi - V_T^\Phi]$  and dividing the simulated  $\mathbb{E}[V_T^\Psi - V_T^\Phi]$  by  $\Delta t^{2H-1}$ , we see that, in our basis setting, this ratio approaches  $C = 106.2$ . This numerically supports our theoretical convergence results.

### 3.3 Discretized Salopek strategy

#### 3.3.1 General strategy behavior

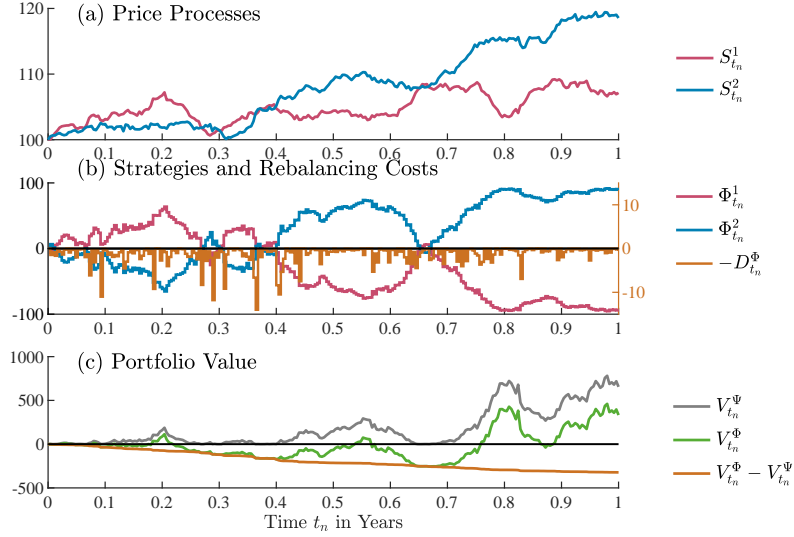
We now turn to the Salopek strategy trading only risky assets and put special emphasis on a simple and practically appealing specification with  $d = 2$  assets.<sup>22</sup> Following our approach for the Shiryaev strategy, Figure 3.8 starts by presenting a typical simulated realization in the basis setting of Table 3.1. This means that we plot the prices  $S_{t_n}^1$  and  $S_{t_n}^2$ , the asset holdings  $\Phi_{t_n}^1$  and  $\Phi_{t_n}^2$ , the negative rebalancing costs  $-D_{t_n}^\Phi$  as well as the discrete and continuous strategy value processes  $V_{t_n}^\Phi$  and  $V_{t_n}^\Psi$  including their differences  $V_{t_n}^\Phi - V_{t_n}^\Psi$ .

In line with Proposition 2.2, we see that the investor is always long (short) in the asset with the higher (lower) price. Because the continuous-time value (2.15) tells us that  $V_t^\Psi = M_\beta(S_t) - M_\alpha(S_t) \geq 0$ , the properties of the  $a$ -order power mean  $M_a(\cdot)$  imply that the portfolio value of the Salopek strategy is all the greater the more the prices of the two assets deviate from each other. If they coincide, we have  $M_\beta(S_t) = M_\alpha(S_t)$  and consequently a  $V_t^\Psi$  of zero. These features are comparable to the Shiryaev strategy.

At first glance, it appears that there are also strong rebalancing cost similarities between the Shiryaev and Salopek strategies. For the Shiryaev strategy, we have shown that the rebalancing costs  $D_{t_n}^\Phi$  are strictly positive for  $n = 1, \dots, N-1$  (see Proposition 3.1). Figure 3.8 suggests the same property for the Salopek strategy.<sup>23</sup> However, this does not hold in general. It can be verified via experiments with different choices of  $(\alpha, \beta)$  that  $D_{t_n}^\Phi$  may be negative for some  $n$  (see, for example, Figure B.1 of the appendix). Thus, in contrast to the

<sup>22</sup> For the strategy to work, the prices of the two assets should not be perfectly correlated. This is ensured by our independence assumption of Section 2.1.

<sup>23</sup> Both strategies have in common that their rebalancing costs tend to be highest when asset prices experience sharp changes and price paths cross.



For the discretized Salopek strategy and our basis setting of Table 3.1, this figure plots a typical simulation result. Panel (a) shows the realized prices  $S_{t_n}^1$  and  $S_{t_n}^2$  of the two risky assets. Panel (b) illustrates the strategy holdings  $\Phi_{t_n}^1$  and  $\Phi_{t_n}^2$  for these assets. Furthermore, it contains the negative rebalancing costs  $-D_{t_n}^\Phi$ . Finally, Panel (c) reports the portfolio value  $V_{t_n}^\Phi$  of the strategy. It is supplemented by the value process  $V_{t_n}^\Psi$  of continuous-time trading and the difference between both portfolio values which, except for terminal time  $t_N = T = 1$ , is equal to the holdings  $\Phi_{t_n}^3$  in the transaction account.

Fig. 3.8: Exemplary realization of the discretized Salopek strategy

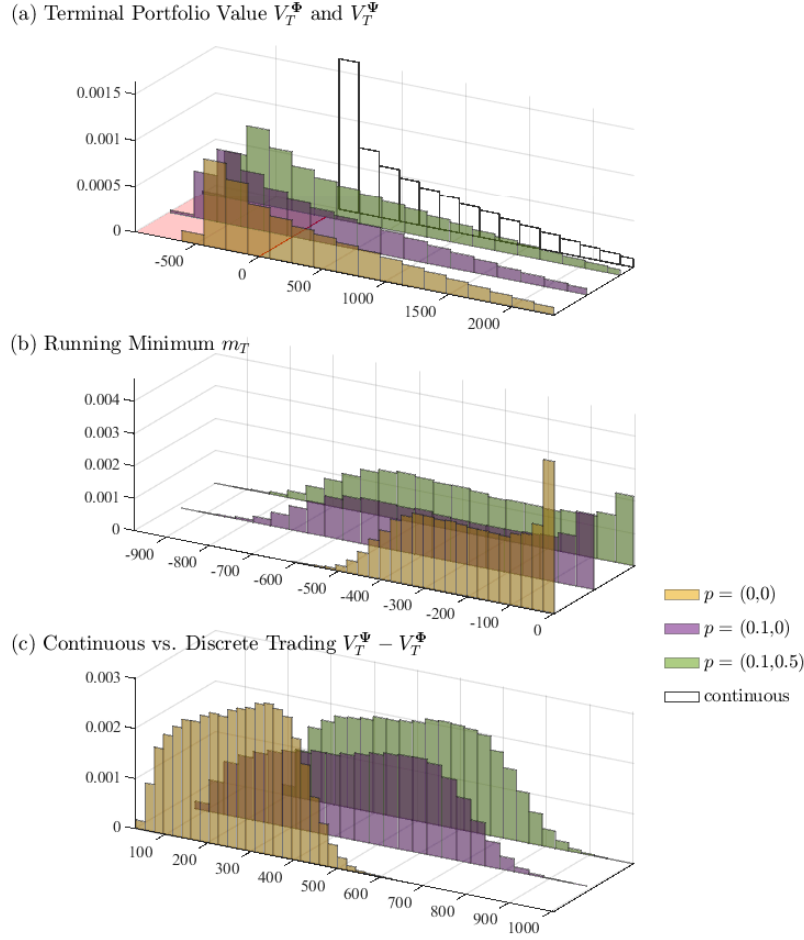
Shiryaev strategy, the portfolio value  $V_{t_n}^\Phi$  of the discretized Salopek strategy can exceed the portfolio value  $V_{t_n}^\Psi$  of its continuous-time counterpart.

### 3.3.2 Impact of time discretization and transaction costs

Uniting all 100,000 simulation scenarios and charging transaction costs in the Salopek strategy, Figure 3.9 presents the distributions of the terminal portfolio values  $V_T^\Psi$  and  $V_T^\Phi$ , the running minimum  $m_T$  and the difference  $V_T^\Psi - V_T^\Phi$ . In addition, Table 3.7 reports summary statistics for the terminal value distributions.

Similar to the Shiryaev case, discretization and transaction costs expand the negative distribution support of  $V_T^\Phi$  and  $m_T$  and increase  $V_T^\Psi - V_T^\Phi$ . However, the Salopek strategy differs in notable aspects. First, without transaction costs, the means of  $V_T^\Psi$  and  $V_T^\Phi$  are 806.3 and 534.1, respectively. Because 534.1 covers just about 66% of 806.3, the Salopek strategy exhibits larger discretization shrinkage than the Shiryaev strategy. The theoretical counterpart of the latter value, delivered by the numerical integration of Remark 2.4, is 805.9. The former quantity can be approximated via Proposition 3.3 which derives a rebalancing cost expansion (under zero transaction costs) with convergence features similar to the Shiryaev Proposition 3.2. It quite accurately yields 537.7 (see also Table 3.8). Second, turning to  $p = (0.1, 0)$ , the terminal mean and loss probability are 349.7 and 47%, respectively. These values are higher than for the Shiryaev strategy but must be put into the perspective that the Salopek strategy drains the transaction account more significantly than the Shiryaev strategy. Finally, for  $p = (0.1, 0.5)$ , we observe a terminal mean of 303.0 accompanied by a loss probability of 48%. While, in the Shiryaev case, the minimum fee causes a negative mean and a very high loss probability, this does not occur for the Salopek





For 100,000 simulated scenarios of the discretized Salopek strategy, the basis setting of Table 3.1 and a range of transaction cost values, this figure presents various portfolio value distributions. Panel (a) shows the distributions of the terminal value  $V_T^\Phi$  of discrete-time trading with transaction costs  $p = (p_1, p_2)$  where  $p_1$  reflects proportional costs (in percent) and  $p_2$  is a minimum fee (in monetary units). The loss region with negative terminal values is highlighted by a red floor. The distribution of the terminal value  $V_T^\Psi$  of continuous-time trading is also included. Panel (b) contains the distributions of the running minimum  $m_T$  of the discrete value processes, i.e., the worst-case portfolio values in the investment horizon. Finally, the distributions in Panel (c) refer to the terminal difference  $V_T^\Psi - V_T^\Phi$  between continuous-time and discrete-time trading. For better visibility, the x-axis in Panel (a) is cut off after the 95% quantile of  $p = (0,0)$ .

Fig. 3.9: Salopek portfolio value distributions for different transaction costs

strategy because of its larger trading volumes. Overall, transaction costs do not diminish the performance of the discretized strategy to a point of financial futility.

**Proposition 3.3 (Expected cumulated Salopek rebalancing costs)** *Assume a market with an equidistant time discretization of step size  $\Delta t > 0$  and consider the discrete-time Salopek strategy with parameters  $\alpha, \beta \in \mathbb{R} \setminus \{0\}, \alpha < \beta$ . Then, for  $\Delta t \rightarrow 0$ , the expectation of its cumulated rebalancing costs  $\mathcal{D}_T = \mathcal{D}_T(\Delta t) = \sum_{n=1}^N D_{t_n}^\Phi$  given in (2.24) satisfies*

$$\mathbb{E}[\mathcal{D}_T(\Delta t)] = C \Delta t^{2H_{\min}-1} + o(\Delta t^{2H_{\min}-1}) \quad \text{with} \quad C = C(\alpha, \beta) = \bar{C}(\beta) - \bar{C}(\alpha),$$

$$\text{where} \quad \bar{C}(a) = \frac{a-1}{2d} \int_0^T \mathbb{E} \left[ M_a(S_t) \sum_{i \in \mathcal{I}_{\min}} (\sigma^i)^2 \left( \frac{S_t^i}{M_a(S_t)} \right)^a \left( 1 - \frac{1}{d} \left( \frac{S_t^i}{M_a(S_t)} \right)^a \right) \right] dt,$$

$$H_{\min} = \min\{H^1, \dots, H^d\}, \quad \mathcal{I}_{\min} = \{i \in \{1, \dots, d\} : H^i = H_{\min}\}.$$

*Proof.* See Appendix A.6.

Strat.	Transact. costs $p$	Mean	Stand. dev.	Min	Quantiles			Max	Loss prob.
					5%	Median	95%		
$\Psi$	none	806.3 (805.9)	817.7 (813.5)	0.0 (0.0)	6.1 (6.7)	551.3 (556.4)	2,462.3 (2,458.6)	6,813.7 ( $\infty$ )	0.00 (0.00)
$\Phi$	(0,0)	534.1	893.6	-609.3	-393.6	273.9	2,322.1	6,682.6	0.37
	(0.1,0)	349.7	940.1	-962.7	-660.3	85.2	2,219.2	6,591.0	0.47
	(0.1,0.5)	303.0	920.3	-977.7	-680.7	42.4	2,136.0	6,492.0	0.48

This table reports some descriptive statistics for the simulated terminal portfolio value distributions in Panel (a) of Figure 3.9. Besides the mean and standard deviation, we compute the minima and maxima as well as selected quantiles. Furthermore, we present the simulated loss probability, i.e., the proportion of negative terminal portfolio values. The numbers in parentheses for the continuous-time portfolio represent theoretical values obtained via the numerical integration of Remark 2.4.

Table 3.7: Salopek portfolio value statistics for different transaction costs

**Remark 3.1** For the special case of  $d$  assets with identical Hurst coefficients and volatilities, i.e.,  $H^i = H, \sigma^i = \sigma, i = 1, \dots, d$ , which we consider in our basis setting, the expression defining  $\bar{C}(a)$  in Proposition 3.3 can be simplified to

$$\bar{C}(a) = \frac{(a-1)\sigma^2}{2} \int_0^T \mathbb{E} \left[ M_a(S_t) \left( 1 - \frac{1}{d} \left( \frac{M_{2a}(S_t)}{M_a(S_t)} \right)^{2a} \right) \right] dt.$$

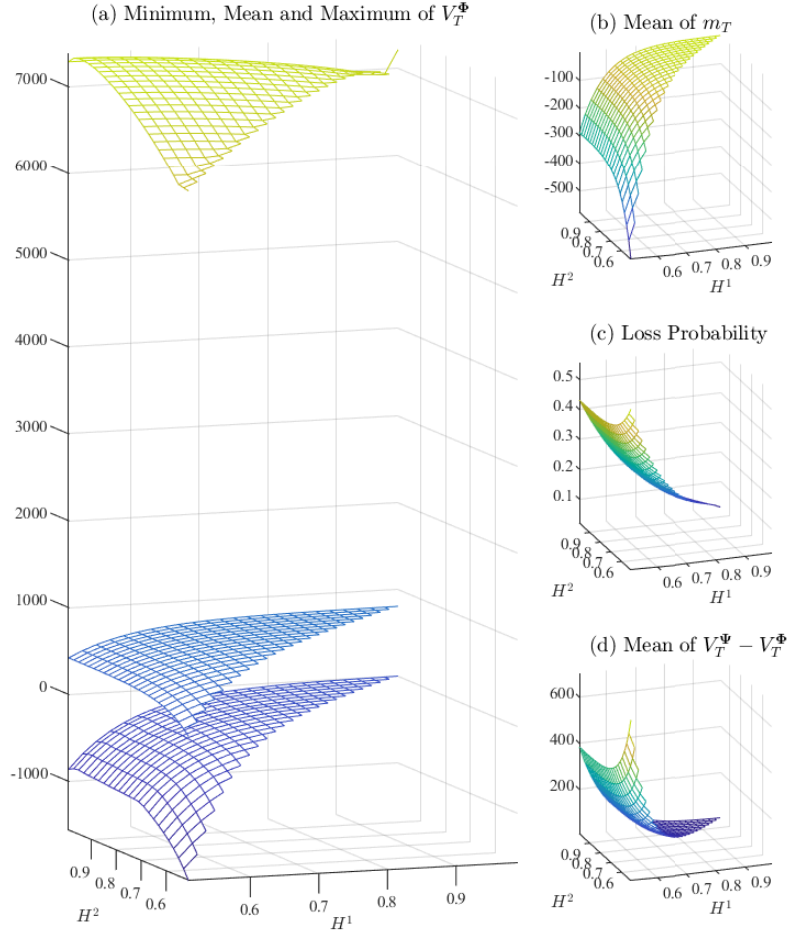
Here, the equality of the drifts  $\mu^1, \dots, \mu^d$  is not required.

### 3.3.3 Impact of Hurst parameters

Our basis setting assumes that the Hurst coefficients of the traded assets are identical, i.e.,  $H^1 = H^2$ . Because this is not a necessary requirement for strategy execution, we also investigate Hurst values of different magnitudes. Given the complexity of this exercise, Figure 3.10 presents its results, i.e., the characteristics of the terminal portfolio value distributions, in three-dimensional form. For  $H^1, H^2 \in [0.51, 0.99]$  with  $H^1 \leq H^2$ , Panel (a) plots the minimum, mean and maximum of  $V_T^\Phi$ .<sup>24</sup> Panels (b), (c) and (d) cover the mean of the running minimum  $m_T$ , the loss probability and the mean of  $V_T^\Psi - V_T^\Phi$ , respectively.

Higher persistence pushes terminal values, limits the risk of loss and reduces capital infusions. If both  $H^1$  and  $H^2$  approach their limit value one, the loss probability and the mean of the running minimum are drawn to zero. Put differently, even though discretization causes  $V_T^\Psi - V_T^\Phi \neq 0$ , the discretized Salopek strategy converges to an almost perfect arbitrage strategy. This can be explained by the limiting behavior of the fBm  $B^H$  for  $H \rightarrow 1$ . In this situation, (2.2) implies for the covariance  $\text{Cov}(B_t^H, B_s^H) \rightarrow ts$  such that  $B_t^H$  and  $B_s^H$  are perfectly positively correlated for all  $t, s > 0$  and it can be deduced that  $B_t^H = tB_1^H$ . Because the fBm is a centered Gaussian process, we obtain  $B_t^{H^i} = Z^i t$  with independent standard Gaussian random variables  $Z^i, i = 1, 2$ . In this case, (2.3) delivers asset prices  $S_t^i = S_0^i \exp\{\mu^i t + \sigma^i Z^i t\}$ . Because their paths are exponential functions with growth rate  $\mu^i + \sigma^i Z^i$ , the quantities  $Z^i$  are the only source of uncertainty. However, they are unveiled to the investor with the asset price observations at the first trading time  $t_1$ . This means that, after  $t_1$ , future asset prices are completely known. If the growth rate of  $S^1$  is above (below) the one of  $S^2$ , we have  $S_t^1 > S_t^2$  ( $S_t^1 < S_t^2$ ) for all  $t \in [0, T]$ . Thus, a long position in the asset with the larger price and a short position in the other is an obviously risk-free strategy.

<sup>24</sup> The outcomes for  $H^1 > H^2$  follow by symmetry.



For 100,000 simulated scenarios of the discretized Salopek strategy, the basis setting of Table 3.1 and a range of Hurst parameter values  $H^1, H^2 \in [0.51, 0.99]$  with  $H^1 \leq H^2$ , this figure characterizes the corresponding distributions of the terminal portfolio value  $V_T^\Phi$ . Panel (a) shows the minimum, mean and maximum of  $V_T^\Phi$ . Panel (b) plots the mean of the running minimum  $m_T$ . Panels (c) and (d) cover the simulated loss probability and the mean of the difference  $V_T^\Psi - V_T^\Phi$  between continuous and discrete trading, respectively.

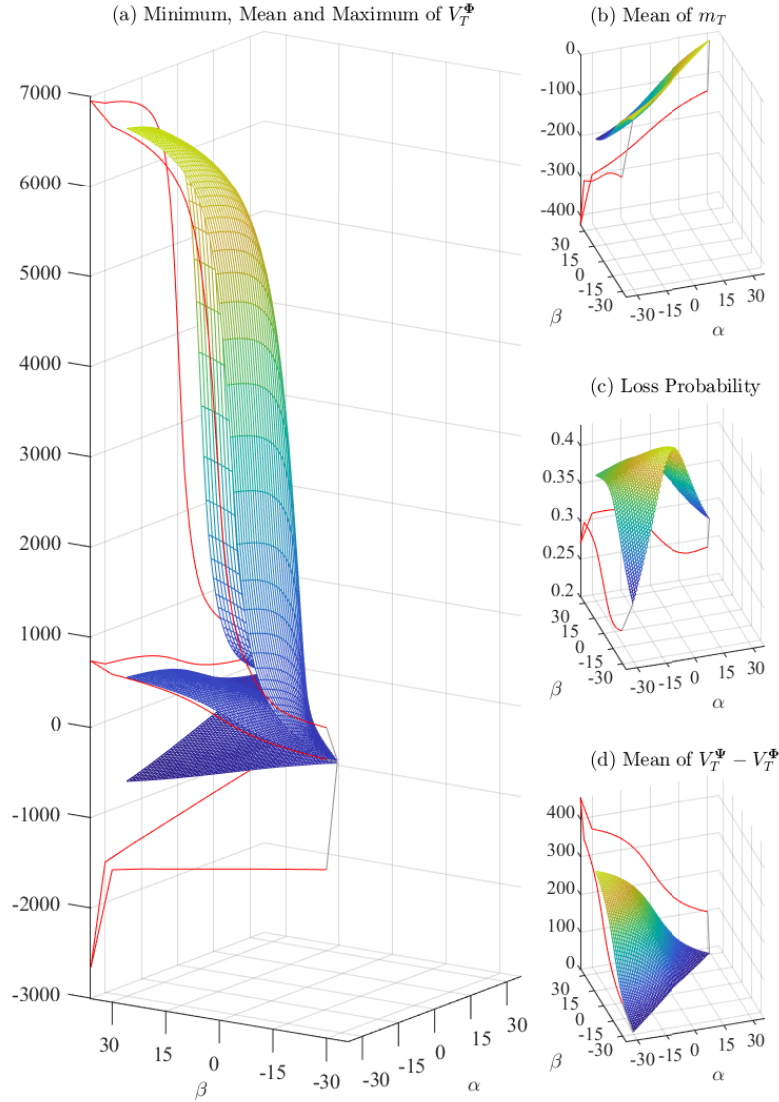
Fig. 3.10: Salopek sensitivity to Hurst coefficients

### 3.3.4 Impact of strategy parameters

While Shiryayev-type investors have access to a unique trading rule, Salopek investors are confronted with a family of rules parameterized by  $(\alpha, \beta)$ . Consequently, they need to choose a suitable tuple  $(\alpha, \beta)$  in practical applications. In the continuous-time case, (2.15) and (2.13) imply that the maximum portfolio value  $V_t^{\Psi, \max} = \max(S_t^1, S_t^2) - \min(S_t^1, S_t^2)$  is attained for the limiting tuple  $(\alpha, \beta) = (-\infty, \infty)$ . With this setup, the strategy representation (2.11) tells us that  $\Psi$  is a *buy-and-hold* strategy with a long position in the high-priced asset financed by short selling the low-priced asset as long as the sign of  $S^1 - S^2$  is unchanged. If a change occurs, i.e., if the price paths cross, the asset roles simply reverse.<sup>25</sup>

Although the infinite setup is appealing from a theoretical point of view, the question arises whether it also maxes out in a discrete environment. Rebalancing costs may vary with  $(\alpha, \beta)$  and suggest a different optimal parameter choice. To provide an answer, Figure 3.11 plots our set of previously used portfolio value characteristics against the parameters  $\alpha \in$

<sup>25</sup> A graphical illustration of this strategy can be found in Figure B.2 of the appendix.



For 100,000 simulated scenarios of the discretized Salopek strategy, the basis setting of Table 3.1 and a range of strategy parameter values  $\alpha \in [-30, 29]$  and  $\beta \in [\alpha + 1, 30]$ , this figure characterizes the corresponding distributions of the terminal portfolio value  $V_T^\Phi$ . Panel (a) shows the minimum, mean and maximum of  $V_T^\Phi$ . Panel (b) plots the mean of the running minimum  $m_T$ . Panels (c) and (d) cover the simulated loss probability and the mean of the difference  $V_T^\Psi - V_T^\Phi$  between continuous and discrete trading, respectively. The red lines represent the results for the limiting cases  $\alpha = -\infty$  and  $\beta = \infty$ .

Fig. 3.11: Salopek sensitivity to strategy parameters

$[-30, 29]$  and  $\beta \in [\alpha + 1, 30]$ . For  $\alpha = \beta$ , the Salopek positions and portfolio value are zero because we are not invested in any risky asset. With growing difference  $\beta - \alpha$ , the means of  $V_T^\Phi$  and  $V_T^\Psi - V_T^\Phi$  increase. They reach their maxima for the limit  $\beta = -\alpha = \infty$ . Thus, even though the rebalancing costs are also at their maximum, continuous-time and discrete-time trading both max in the same limiting case. With respect to the loss probabilities, we observe values between 23% and 43%. The highest probability arises for the tuple  $(\alpha, \beta) = (0, 1)$ , the lowest for  $(20, \infty)$ . In the case of  $\beta = -\alpha = \infty$ , we have 27%.

Investors basically have two well-known options when setting their individual  $(\alpha, \beta)$ . First, they may tune the parameters by determining the values that optimize a given target function (or a set of target functions). For example, the reward earned per unit of investment

risk could be maximized (see Xiang and Deng, 2024). Such an endeavor yields diverse results because the literature offers a wide variety of alternative reward-to-risk ratios (see Rachev et al., 2007; Eling and Schuhmacher, 2007). Second, and very popular in practice, a sequential approach is feasible. That is, investors use visualizations like Figure 3.11 to check whether a desired reward goes along with personally acceptable risk and budget levels (see Bodie et al., 2009). If it does, the corresponding parameters are chosen. Otherwise, the reward must be adjusted to meet risk and budget preferences.

### 3.3.5 Impact of trading horizon and frequency

To complete our analysis of the Salopek strategy, we study its sensitivity to different trading horizons and frequencies and compare the findings to the Shiryayev strategy.

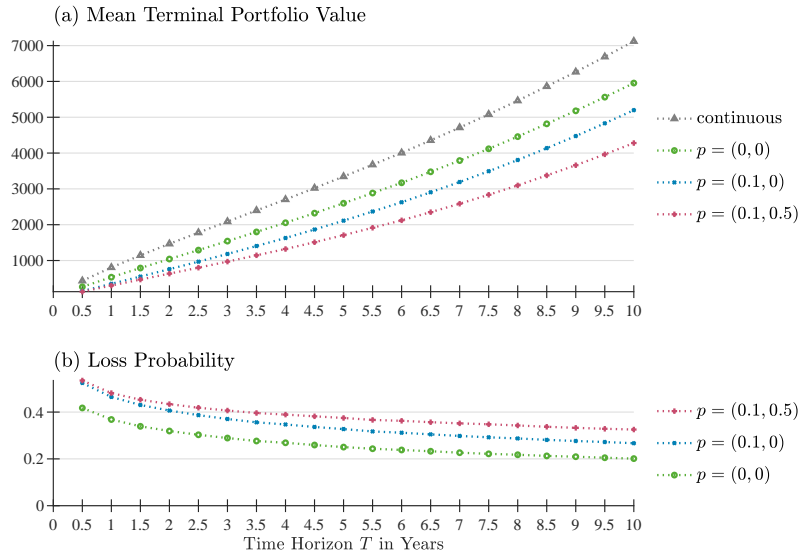
**Trading horizon.** Again, we start by enlarging the trading horizon  $T$  and upholding a daily trading frequency. For our three transaction cost variants, Figure 3.12 displays the mean terminal portfolio value and the loss probability as functions of  $T$ . For both  $\Psi$  and  $\Phi$ , Panel (a) suggests that the growth of the mean terminal values in the first ten years is only slightly faster than linear. This is in contrast to the Shiryayev strategy where we detected faster than exponential growth. While, for smaller  $T$ , the means of the Salopek strategy are larger than those of the Shiryayev strategy, the latter surpass the former for higher  $T$ . In particular, for  $T = 10$ , the Shiryayev values exceed the Salopek values nearly twofold. In our drifting environment, this can be linked to the fact that the Shiryayev asset tends to deviate further from its initial price than the Salopek assets deviate from each other. Panel (b) shows that the loss probabilities decrease with  $T$ . While the Salopek strategy has some comparative advantages in the short run and the minimum fee setting, the Shiryayev strategy stands out in the long run. In particular, for  $T = 10$  and proportional costs, the former is not as close to 20% as the latter. Moreover, with rising  $T$ , the Salopek probabilities related to minimum fee transaction costs do not approach those of purely proportional costs.

**Trading frequency.** Figure 3.13 sets diverse trading frequencies within a locked trading horizon of  $T = 1$  year. The resulting mean terminal portfolio values in Panel (a) imply that, even in the presence of transaction costs, higher trading frequencies are beneficial for investors. In contrast to the Shiryayev strategy, the impact of minimum fees at high frequencies is almost negligible. The loss probabilities in Panel (b) also recommend more frequent trading. The value of 37% for fee-less daily trading illustrates once more that unavoidable rebalancing costs in discrete-time trading induce losses that prevent the strategy from reaching the zero probability limit of an infinite trading frequency.

Finally, similar to the Shiryayev investigation, Table 3.8 studies the approximation accuracy and the convergence speed of the expansion in Proposition 3.3. The proxy proves to be very useful because the deviations between simulated and approximated values range from roughly 6% at low frequency ( $N = 12$ ) to about 0.25% at high frequency ( $N = 250$ ). In addition, the proposed convergence rate  $C$  and order  $2H - 1$  are nicely confirmed by our simulation exercise.

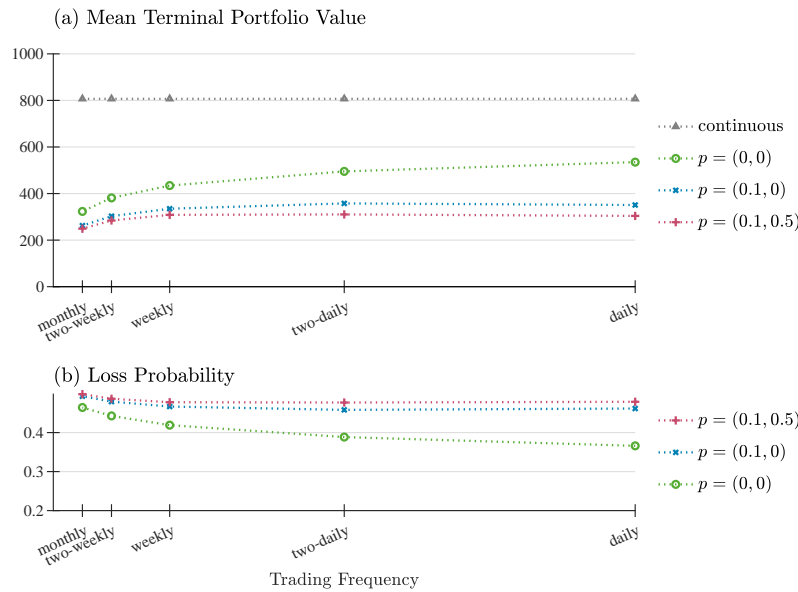
## 4 Empirical illustration

To complete our study, we leave the simulation setup with artificially generated data and shed some light on the implementation and performance of the Shiryayev and Salopek strate-



For 100,000 simulated scenarios of the discretized Salopek strategy, the basis setting of Table 3.1 and a range of transaction cost values  $p$ , this figure plots (a) the mean of the terminal portfolio value and (b) the simulated loss probability against the trading horizon  $T$ . The continuous case is included as a reference.

Fig. 3.12: Salopek sensitivity to trading horizon



For 100,000 simulated scenarios of the discretized Salopek strategy, the basis setting of Table 3.1 and a range of transaction cost values  $p$ , this figure plots (a) the mean of the terminal portfolio value and (b) the simulated loss probability against the trading frequency. The continuous case is included as a reference.

Fig. 3.13: Salopek sensitivity to trading frequency

gies in empirical data. Specifically, we obtain an illustrative data set from Refinitiv Eikon which spans from January 2013 to December 2023 and covers daily price information of the 1,689 full-history stocks listed in the 41 country subindices of the Datastream Emerging

Frequency	$N$	$\mathbb{E}[V_T^\Phi]$		$(\mathbb{E}[V_T^\Psi - V_T^\Phi]) / \Delta t^{2H-1}$ simulated
		simulated	approximated	
Monthly	12	323.2	304.6	794.1
Two-weekly	25	381.3	373.0	809.1
Weekly	50	434.3	429.0	813.5
Two-daily	125	494.2	492.1	817.1
Daily	250	534.1	532.7	821.3
	$\infty$	806.3	$\mathbb{E}[V_T^\Psi] = 805.9$	$C = 824.0$

For several trading frequencies of the Salopek strategy and the basis setting of Table 3.1, this table contrasts the simulated and the approximated values of  $\mathbb{E}[V_T^\Phi]$  where the latter are obtained via Proposition 3.3. The numbers in the last line represent the simulated and exact values of  $\mathbb{E}[V_T^\Psi]$  taken from Table 3.7. The last table column divides the simulated value of  $\mathbb{E}[V_T^\Psi - V_T^\Phi]$  by  $\Delta t^{2H-1}$ .  $C$  is the rate of convergence in Proposition 3.3.

Table 3.8: Salopek mean approximation

Market Index.<sup>26</sup> In this asset universe, we then conduct an rolling window analysis which is an established standard in investment research and practice because it avoids look-ahead bias with respect to asset selection criteria and can take into account the time-varying nature of memory effects and other return properties (see Mehlich and Auer, 2024).

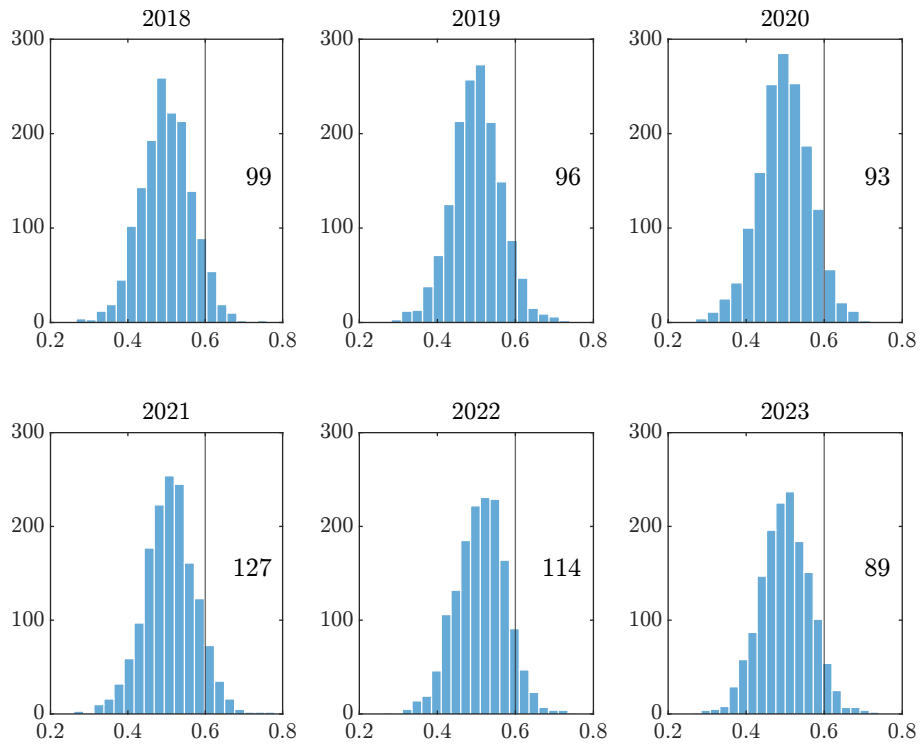
We opt for annually rolling a five-year data window. This means that, at the beginning of each year between 2018 and 2023, we have to use data of the preceding five years to determine which stocks are eligible to enter our strategies. Specifically, we need to know which of them are compatible with a fBm exhibiting  $H > 0.5$ .<sup>27</sup> Unfortunately, the current state of the statistical literature does not supply procedures that can reliably test for fBm behavior, i.e., simultaneously verify the validity of the model and estimate its parameters (see Sikora, 2018). Therefore, we follow a heuristic approach popular in empirical research. That is, we deduce the fBm property from previous studies persuasively suggesting predictable variation in emerging market equities (see Wilcox and Gebbie, 2008) and consider a measured  $H$  to be economically relevant if it exceeds 0.6 (see Batten et al., 2013). To estimate the Hurst coefficient of a stock with the window data, we use the traditional rescaled range method (see Weron, 2002) because it is fairly robust to short time-series, short-term memory and non-normality (see Chamoli et al., 2007; Kristoufek, 2012).<sup>28</sup> Based on the obtained estimates, we exclude stocks with  $H$  values below 0.6. The remaining stocks are then rebased to one and traded for a one-year horizon and on a daily frequency. As far as the strategy specifications are concerned, we use  $p = (0.1, 0)$ ,  $\gamma = 10^2$  and  $(\alpha, \beta) = (-30, 30)$ . While the Shiryaev strategy is implemented for each stock, the Salopek strategy considers all possible pairs of stocks.

Figures 4.1 and 4.2 present our results. For each investment period, Figure 4.1 plots the distribution of Hurst coefficient estimates over all stocks and highlights the ones that we consider appropriate for our strategies. Interestingly, this only applies to a small fraction of stocks. For example, while we can invest in 99 stocks in 2018, we have 127 in 2021.

<sup>26</sup> The request mnemonic for this data is G#LTOTMKEK0424. In additional calculations with developed market equities (i.e., the constituents of the DAX 40, EURO STOXX 50, FTSE 100, and S&P 500), we attained notably weaker results.

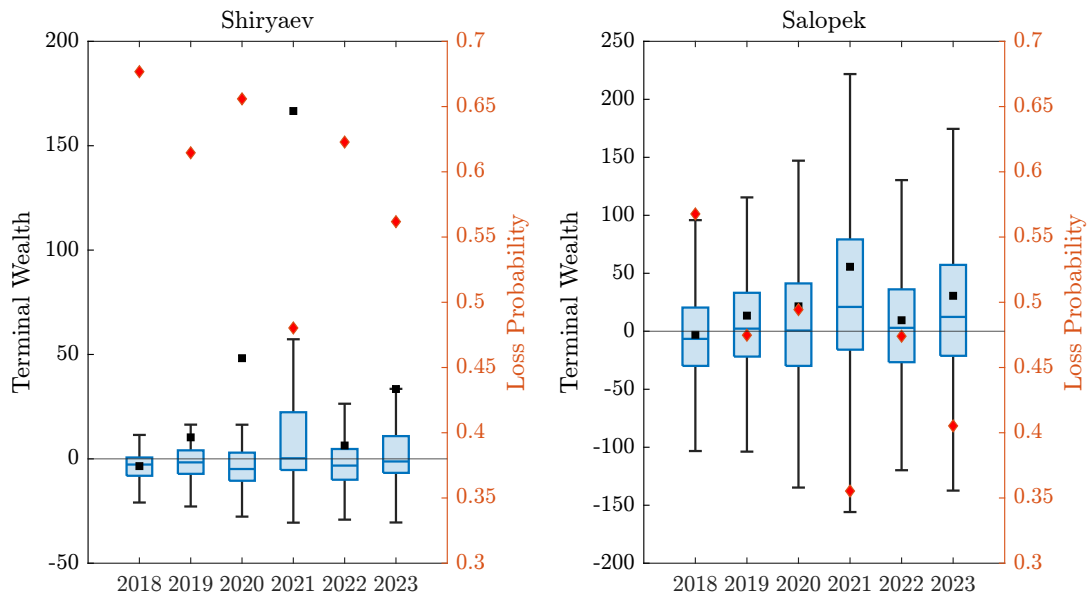
<sup>27</sup> As stated in Appendix C, our specific strategies only hold for the case  $H > 0.5$  where the fBm features zero quadratic variation. Investors interested in exploiting  $H < 0.5$ , where the quadratic variation of the fBm is infinite (see Biagini et al., 2008), may turn to the strategies of Garcin (2022) and Xiang and Deng (2024).

<sup>28</sup> Note that rescaled range analysis should utilize logarithmic instead of simple returns (see Auer, 2016).



For each investment period in our sample, this figure displays the distribution of emerging market equity Hurst coefficient estimates. Estimation is performed by traditional rescaled range analysis and a daily return data window covering the five years prior to the investment period. The numbers within the figures show how many stocks satisfy  $H \geq 0.6$ , i.e., enter our investment strategies.

Fig. 4.1: Empirical Hurst coefficient values



For each investment period in our sample, this figure visualizes the performance of the Shiryayev and Salopek strategies for the persistent stocks and stock pairs identifiable via Figure 4.1. Recall that we trade daily over one year, use a rebasing to one and set  $p = (0.1, 0)$ ,  $\gamma = 10^2$  and  $(\alpha, \beta) = (-30, 30)$ . Besides presenting the terminal wealth distributions in the form of Box-Whisker plots, we report the mean terminal value (black rectangles, left axis) and the empirical loss probabilities (red diamonds, right axis) of the strategies.

Fig. 4.2: Empirical strategy performance



Using these stocks in the Shiryaev and Salopek strategies delivers the outcomes summarized in Figure 4.2. It yearly visualizes the terminal wealth distributions of the strategies in the form of Box-Whisker plots. In addition, it provides the mean terminal wealth and the empirical loss probability. For the Shiryaev strategy, we observe that, with the exception of 2018, it generates positive terminal values on average which are accompanied by rather high loss probabilities. In comparison, the Salopek strategy shows the same mean terminal wealth signs but at significantly lower loss probabilities. Both strategies perform best in the year 2021.<sup>29</sup> The apparently time-varying performance of the strategies can be explained by various factors including parameter instability and randomness. Most importantly, our samples may still contain stocks which cannot be adequately described by a fBm.

## 5 Conclusion

In this study, we have revisited the arbitrage strategies of Shiryaev (1998) and Salopek (1998) because they have a solid theoretical foundation and an elegant intuitive design making them interesting for investment practice. While the Shiryaev strategy trades only one risky asset and benefits from both rising and falling prices, the most elementary specification of the Salopek strategy trades two risky assets and capitalizes on prices drifting apart. Both strategies have very simple trading rules and rely only on realized prices, which are readily available in today's investment world, so that they can be easily automated in modern algorithmic trading facilities.

Because these strategies aim at continuous-time trading in a fractional Black-Scholes market, we have transferred them to a discrete-time application and intensively studied their investment performance via Monte Carlo simulation and formal mathematical approximation. In conservative settings with independent assets, moderate serial correlation and realistic transaction costs, we show that, even though they can no longer be considered as arbitrage strategies, they exhibit positive terminal values on average and are accompanied by low loss probabilities. This makes them particularly interesting for tail-oriented investors (see Gao et al., 2018). Furthermore, we have revealed several interesting features of the discretized strategies. First, they perform reasonably well even if assets show relatively small persistence. Second, certain limiting cases of the strategies not only max out their performance but further simplify their implied asset positions. Third, time-discretization does not necessarily lead to portfolio values lower than in the continuous-time case. Finally, when adequately scaled, the strategies are useful for short-, medium- and long-term horizons and most advisable at a daily trading frequency. This nicely integrates into the growing literature on the welfare consequences of speeding up transactions in financial markets (see Du and Zhu, 2017).

Our study offers plenty of scope for future research. With respect to theoretical work, it is instructive to introduce an interest-bearing transaction account (with potentially differing rates for borrowing and lending) and to consider the market impact of large-scale trades (see Guasoni et al., 2019, 2021). Furthermore, modeling a negative cross-correlation between risky assets can be considered a fruitful endeavor because it has the potential to increase strategy performance. It also makes the strategies comparable to the domain of pairs trading rules for correlated assets (see Krauss, 2017; Chen et al., 2017). Finally, while we

---

<sup>29</sup> The outstanding Shiryaev mean in this year is largely caused by about 20 stocks with exceptional strategy performance outside the plot quantile range.

have focused on the usefulness of the strategies in their originally proposed form, it is worth investigating whether they can be improved by modifications and how they perform in a direct comparison with related strategies (see Garcin, 2022; Xiang and Deng, 2024). Potential modifications include strategy starting points updated during the investment life cycle, early liquidation rules (e.g., closing when a given minimum gain has been achieved), lock-in mechanisms partially securing ongoing profits (e.g., shorting when the price falls below half of the maximum reached) and adapted time grids (e.g., optimal hitting-based rebalancing instead of rigid end-of-period trading). As far as empirical work is concerned, we suggest an extension of our brief empirical illustration to a profound analysis of the Shiryaev and Salopek strategies in different asset classes and markets. Besides emerging market equities, currency investments are a particularly promising playground for such an endeavor because exchange rates show pronounced periodic smoothness, memory and predictability (see Karemera and Kim, 2006; Hassan and Mano, 2019). Similar statements can be made for stable evolutions in (investment grade) corporate bond prices. However, taking this path requires overcoming the obstacle of sound fBm testing. To achieve this, one could sequentially apply test procedures constructed for a given hypothetical  $H$  (see Sikora, 2018). Alternatively, these techniques might be suitably combined with a pre-estimate or a concurrent estimation of  $H$  based on methods more advanced than rescaled range analysis (see López-Garíca et al., 2021). Only this way it is possible to reliably answer the question of whether an asset qualifies for our memory-based investment strategies.

## Appendix

### A Proofs

#### A.1 Proof of Proposition 2.1

*Proof.* We use expression (2.9) for the portfolio value of the Shiryaev strategy and the price model (2.3). They yield

$$V_T^\Psi = \frac{1}{s_0^1} (S_T^1 - s_0^1)^2 = s_0^1 (\exp\{\mu T + \sigma B_T^H\} - 1)^2 = s_0^1 (e^Z - 1)^2 = s_0^1 (e^{2Z} - 2e^Z + 1).$$

Here,  $Z = \mu T + \sigma B_T^H$  is a Gaussian random variable with mean  $\mu T$  and variance  $\sigma^2 T^{2H}$ . Hence,  $e^{2Z}$  and  $e^Z$  are lognormally distributed. Taking expectation provides the proposed expression for  $\mathbb{E}[V_T^\Psi]$ . The proof for  $\mathbb{E}[(V_T^\Psi)^2]$  is similar. The variance follows from Steiner's formula. For the cumulative distribution function of  $V_T^\Psi$  with  $v \geq 0$ , we have

$$\begin{aligned} F_{V_T^\Psi}(v) &= \mathbb{P}(V_T^\Psi \leq v) = \mathbb{P}(s_0^1 (e^Z - 1)^2 \leq v) = \mathbb{P}\left(-\sqrt{v/s_0^1} \leq e^Z - 1 \leq \sqrt{v/s_0^1}\right) \\ &= \mathbb{P}\left(\log \left\{ \left(1 - \sqrt{v/s_0^1}\right)^+ \right\} \leq Z \leq \log \left\{ 1 + \sqrt{v/s_0^1} \right\}\right). \end{aligned}$$

Since  $Z \sim \mathcal{N}(u, s^2)$  with  $u = \mu T$  and  $s = \sigma T^H$ , the claim follows from  $\mathbb{P}(a \leq Z \leq b) = \bar{\Phi}((b - u)/s) - \bar{\Phi}((a - u)/s)$  for  $a \leq b$ .  $\square$

#### A.2 Proof of Lemma 2.1

*Proof.* Based on the transaction account recursion (2.21), we infer (2.24) from (2.23). To show that (2.24) also holds at liquidation, we use (2.21) and the revenue expression (2.19) to obtain

$$V_T^\Phi = R^\Phi + \Phi_N^{d+1} = \sum_{i=0}^d \Phi_N^i S_T^i - \sum_{n=1}^{N-1} D_{t_n}^\Phi - \mathcal{L}_T. \quad (\text{A.1})$$

Taking into account that  $\Phi_N = \Psi_{t_{N-1}}$ , we have

$$\sum_{i=0}^d \Phi_N^i S_T^i = \sum_{i=0}^d \Psi_{t_{N-1}}^i S_T^i = \sum_{i=0}^d \Psi_T^i S_T^i - D_{t_N}^\Phi = V_T^\Psi - D_{t_N}^\Phi, \quad (\text{A.2})$$

where  $D_{t_N}^\Phi = \sum_{i=0}^d (\Psi_{t_N}^i - \Psi_{t_{N-1}}^i) S_T^i$  follows the rebalancing cost definition  $D_{t_n}^\Phi$ ,  $n = 1, \dots, N-1$ , in (2.20) but is now evaluated at terminal time  $t_N = T$ . Because there is no further rebalancing at time  $T$ , these costs may be called ‘‘virtual costs’’. They are not booked to the transaction account. Substituting (A.2) into (A.1) yields  $V_T^\Psi - V_T^\Phi = \mathcal{D}_T + \mathcal{L}_T$  and proves the validity of (2.24) for  $t = T$ . Here,  $\mathcal{D}_T$  is defined as in (2.24). It represents the cumulated rebalancing costs over the entire trading period  $[0, T]$  including the virtual cost term  $D_{t_N}^\Phi$ .  $\square$

### A.3 Proof of Proposition 2.2

*Proof.* Recall the Salopek strategy (2.11) where  $\Psi_t^i(\alpha, \beta) = \widehat{\Psi}_t^i(\beta) - \widehat{\Psi}_t^i(\alpha)$ ,  $\widehat{\Psi}_t^i(a) = \frac{1}{d} \left( \frac{S_t^i}{M_a(S_t)} \right)^{a-1}$ , and  $M_a(x)$  is the (2.12)  $a$ -order power mean of  $x = (x^1, \dots, x^d) \in \mathbb{R}_+^d$ .

We start with proving  $\Psi_t^i(\alpha, \beta) > 0$ . Denoting  $x = S_t^i/M_\beta(S_t)$  and  $y = S_t^i/M_\alpha(S_t)$ , relation (2.16) implies  $1 < x < y$  and  $\beta \geq 1 > \alpha$  gives  $x^{\beta-1} \geq 1 > y^{\alpha-1}$ . Hence,  $(S_t^i/M_\beta(S_t))^{\beta-1} > (S_t^i/M_\alpha(S_t))^{\alpha-1}$ . This proves  $\widehat{\Psi}_t^i(\beta) > \widehat{\Psi}_t^i(\alpha)$  from which the claim follows.

The proof of  $\Psi_t^j(\alpha, \beta) < 0$  is similar. Denoting  $x = S_t^j/M_\beta(S_t)$  and  $y = S_t^j/M_\alpha(S_t)$ , relation (2.16) implies  $0 < x < y < 1$  and  $\beta \geq 1 > \alpha$  gives  $x^{\beta-1} \leq 1 < y^{\alpha-1}$ . Hence,  $(S_t^j/M_\beta(S_t))^{\beta-1} < (S_t^j/M_\alpha(S_t))^{\alpha-1}$ . This proves  $\widehat{\Psi}_t^j(\beta) < \widehat{\Psi}_t^j(\alpha)$  from which the claim follows.

For the special case  $S_t^i = S_t^{i \max} = \max\{S_t^1, \dots, S_t^d\}$  and  $S_t^j = S_t^{j \min} = \min\{S_t^1, \dots, S_t^d\}$ , the monotonicity property (2.13) of the  $a$ -order power mean  $M_a(S_t)$  saying that  $S_t^{\min} \leq M_\alpha(S_t) \leq M_\beta(S_t) \leq S_t^{\max}$  implies (2.16). This completes the proof.  $\square$

### A.4 Proof of Proposition 3.1

*Proof.* Substituting the Shiryaev strategy (2.8) into (2.20) and using  $\Phi_n^i = \Psi_{t_{n-1}}^i$ ,  $n = 1, \dots, N$ , we have almost surely

$$\begin{aligned} D_{t_n}^\Phi &= \frac{(S_{t_{n-1}}^1)^2 - (S_{t_n}^1)^2}{s_0^1} S_{t_n}^0 + \frac{2}{s_0^1} (S_{t_n}^1 - S_{t_{n-1}}^1) S_{t_n}^1 \\ &= \frac{1}{s_0^1} ((S_{t_n}^1)^2 + (S_{t_{n-1}}^1)^2 - 2S_{t_n}^1 S_{t_{n-1}}^1) = \frac{(S_{t_n}^1 - S_{t_{n-1}}^1)^2}{s_0^1} > 0. \end{aligned} \quad \square$$

### A.5 Proof of Proposition 3.2

*Proof.* Based on Proposition 3.1, i.e., expression (3.1) for the rebalancing costs  $D_{t_n}^\Phi$  of the Shiryaev strategy, the cumulative rebalancing costs are given by

$$\mathcal{D}_T(\Delta t) = \sum_{n=1}^N D_{t_n}^\Phi = \frac{1}{s_0^1} \sum_{n=1}^N \mathcal{G}(t_{n-1}, \Delta t) \quad \text{with} \quad \mathcal{G}(t, \Delta t) = (S_{t+\Delta t}^1 - S_t^1)^2, \quad t \in [0, T - \Delta t]. \quad (\text{A.3})$$

We now analyze the asymptotic behavior of  $\mathcal{G}(t, \Delta t)$  for  $\Delta t \rightarrow 0$ . Applying the Taylor expansion  $e^x = 1 + x + O(x^2)$  for  $x \rightarrow 0$  to the increments of the price process (2.3), we obtain

$$\begin{aligned} S_{t+\Delta t}^1 - S_t^1 &= S_t^1 (\exp\{\mu\Delta t + \sigma\Delta B_t^H\} - 1) \\ &= S_t^1 (\mu\Delta t + \sigma\Delta B_t^H + O(\Delta t^2) + O((\Delta B_t^H)^2) + O(\Delta t\Delta B_t^H)), \end{aligned}$$

where we have introduced the shorthand notation  $\Delta B_t^H = B_{t+\Delta t}^H - B_t^H$ . Substituting this expansion into (A.3), taking expectation, and considering that  $\Delta B_t^H \sim \mathcal{N}(0, \Delta t^{2H})$  implies  $\mathbb{E}[(\Delta B_t^H)^2] = \Delta t^{2H}$  and  $\mathbb{E}[(\Delta B_t^H)^k] = o(\Delta t^{2H})$  for  $k \geq 3$ , it follows that

$$\mathbb{E}[\mathcal{G}(t, \Delta t)] = \mathbb{E}[e^{2\sigma B_t^H} (\Delta B_t^H)^2] \sigma^2 (s_0^1)^2 e^{2\mu t} + o(\Delta t^{2H}). \quad (\text{A.4})$$

Here, we have used the boundedness of the moments of  $S_t^1 = s_0^1 \exp\{\mu t + \sigma B_t^H\}$ . The expectation on the r.h.s. of (A.4) can be rewritten as  $\mathbb{E}[e^{Z_1} Z_2^2]$ , where  $Z_1 = 2\sigma B_t^H$  and  $Z_2 = \Delta B_t^H$  form a zero-mean Gaussian random vector  $(Z_1, Z_2)^\top$  with variances  $\mathbb{E}[Z_1^2] = 4\sigma^2 t^{2H}$  and  $\mathbb{E}[Z_2^2] = \Delta t^{2H}$ . For the covariance, (2.2) implies

$$\begin{aligned} \text{Cov}(Z_1, Z_2) &= 2\sigma \text{Cov}(B_t^H, B_{t+\Delta t}^H - B_t^H) = \sigma((t + \Delta t)^{2H} - t^{2H} - \Delta t^{2H}) \\ &= 2\sigma H t^{2H-1} \Delta t + O(\Delta t^{2H}). \end{aligned} \quad (\text{A.5})$$

Applying Isserli's theorem for the computation of the moments of a zero-mean Gaussian vector (see Michalowicz et al., 2009), some algebra delivers, for the r.h.s. expectation of (A.4), the expression

$$\begin{aligned} \mathbb{E}[e^{2\sigma B_t^H} (\Delta B_t^H)^2] &= \mathbb{E}[e^{Z_1} Z_2^2] = (\mathbb{E}[Z_2^2] + (\text{Cov}(Z_1, Z_2))^2) \mathbb{E}[e^{Z_1}] \\ &= (\Delta t^{2H} + O(\Delta t^2)) \mathbb{E}[e^{2\sigma B_t^H}] = \exp\{2\sigma^2 t^{2H}\} \Delta t^{2H} + O(\Delta t^2), \end{aligned}$$

where we have taken into account the expansion (A.5) for  $\text{Cov}(Z_1, Z_2)$ , and that  $e^{2\sigma B_t^H}$  is lognormally distributed with mean  $\exp\{2\sigma^2 t^{2H}\}$ . Substituting into (A.4) and (A.3) yields

$$\begin{aligned} \mathbb{E}[\mathcal{D}_T(\Delta t)] &= \frac{1}{s_0^1} \sum_{n=1}^N \left( \sigma^2 (s_0^1)^2 e^{2\mu t_{n-1}} \exp\{2\sigma^2 t_{n-1}^{2H}\} \Delta t^{2H} + o(\Delta t^{2H}) \right) \\ &= s_0^1 \sigma^2 \frac{1}{\Delta t} \left( \int_0^T \exp\{2\mu t + 2\sigma^2 t^{2H}\} dt + O(\Delta t) \right) \left( \Delta t^{2H} + o(\Delta t^{2H}) \right). \end{aligned}$$

In this context, we have exploited the linear approximation order of the composite rectangular rule applied to the integral  $\int_0^T \exp\{2\mu t + 2\sigma^2 t^{2H}\} dt$ . Multiplying out the brackets proves the claim.  $\square$

### A.6 Proof of Proposition 3.3

*Proof.* Recall the Salopek strategy definition in (2.11). We have  $\Psi_t^i = \Psi_t^i(\alpha, \beta) = \widehat{\Psi}_t^i(\beta) - \widehat{\Psi}_t^i(\alpha)$ ,  $i = 1, \dots, d$ , where  $\widehat{\Psi}_t^i(a) = \frac{1}{d} \left( \frac{S_t^i}{M_a(S_t)} \right)^{a-1}$ , and  $M_a(S_t)$  is the  $a$ -order power mean of  $S_t$ . Using expression (2.20) for the rebalancing costs  $D_{t_n}^\Phi$ , the cumulative rebalancing costs are given by

$$\mathcal{D}_T(\Delta t) = \sum_{n=1}^N D_{t_n}^\Phi = \sum_{n=1}^N \sum_{i=1}^d (\Psi_{t_n}^i - \Psi_{t_{n-1}}^i) S_{t_n}^i = \sum_{n=1}^N \mathcal{H}(t_{n-1}, \beta, \Delta t) - \mathcal{H}(t_{n-1}, \alpha, \Delta t) \quad (\text{A.6})$$

$$\text{with } \mathcal{H}(t, a, \Delta t) = \sum_{i=1}^d (\widehat{\Psi}_{t+\Delta t}^i(a) - \widehat{\Psi}_t^i(a)) S_{t+\Delta t}^i, \quad t \in [0, T - \Delta t], \quad a \in \mathbb{R}.$$

We now analyze the asymptotic behavior of  $\mathcal{H}(t, a, \Delta t)$  for  $\Delta t \rightarrow 0$ . Applying the Taylor expansion  $e^x = 1 + x + x^2/2 + O(x^3)$  for  $x \rightarrow 0$  to the price process (2.3) yields

$$\begin{aligned} \frac{S_{t+\Delta t}^i}{S_t^i} &= \exp\{\mu^i \Delta t + \sigma^i (B_{t+\Delta t}^{H^i} - B_t^{H^i})\} \\ &= 1 + \mu^i \Delta t + \sigma^i \Delta B_t^{H^i} + \frac{1}{2} (\sigma^i)^2 (\Delta B_t^{H^i})^2 + O(\Delta t^2) + O(\Delta t \Delta B_t^{H^i}), \end{aligned} \quad (\text{A.7})$$

where we have introduced the shorthand notation  $\Delta B_t^{H^i} = B_{t+\Delta t}^{H^i} - B_t^{H^i}$ . It holds that

$$\begin{aligned} \mathcal{H}(t, a, \Delta t) &= \sum_{i=1}^d \widehat{\Psi}_{t+\Delta t}^i(a) S_{t+\Delta t}^i - \sum_{i=1}^d \widehat{\Psi}_t^i(a) S_t^i \frac{S_{t+\Delta t}^i}{S_t^i} \\ &= \frac{1}{dM_a^{a-1}(S_{t+\Delta t})} \sum_{i=1}^d (S_{t+\Delta t}^i)^{a-1} S_{t+\Delta t}^i \\ &\quad - \frac{1}{dM_a^{a-1}(S_t)} \sum_{i=1}^d (S_t^i)^{a-1} S_t^i \left(1 + \frac{1}{2} (\sigma^i)^2 (\Delta B_t^{H^i})^2\right) - \mathcal{R}(t, a, \Delta t) \\ &= M_a(S_{t+\Delta t}) - M_a(S_t) - \frac{1}{2dM_a^{a-1}(S_t)} \sum_{i=1}^d (S_t^i)^a (\sigma^i)^2 (\Delta B_t^{H^i})^2 - \mathcal{R}(t, a, \Delta t), \end{aligned} \quad (\text{A.8})$$

where the remainder term is given by

$$\mathcal{R}(t, a, \Delta t) = \frac{1}{dM_a^{a-1}(S_t)} \sum_{i=1}^d (S_t^i)^a \left( \mu^i \Delta t + \sigma^i \Delta B_t^{H^i} + O(\Delta t^2) + O(\Delta t \Delta B_t^{H^i}) \right). \quad (\text{A.9})$$

Next, we derive an asymptotic expansion of the first term in (A.8), i.e., the power mean  $M_a(S_{t+\Delta t})$ , around the point  $S_t$  using the Taylor expansion in (A.7). We have

$$\begin{aligned} M_a(S_{t+\Delta t}) &= \left( \frac{1}{d} \sum_{i=1}^d (S_{t+\Delta t}^i)^a \right)^{1/a} = \left( \frac{1}{d} \sum_{i=1}^d (S_t^i)^a + \Delta Y \right)^{1/a} = (M_a^a(S_t) + \Delta Y)^{1/a} \\ \text{with } \Delta Y &= \frac{1}{d} \sum_{i=1}^d (S_t^i)^a \left( a\mu^i \Delta t + a\sigma^i \Delta B_t^{H^i} + \frac{a^2}{2} (\sigma^i)^2 (\Delta B_t^{H^i})^2 + O(\Delta t^2) + O(\Delta t \Delta B_t^{H^i}) \right). \end{aligned}$$

The second-order Taylor expansion of the function  $x \mapsto f(x) = x^{1/a}$  defined on  $(0, \infty)$  around the point  $x = x_0 > 0$

$$f(x_0 + \Delta x) = x_0^{1/a} \left( 1 + \frac{1}{ax_0} \Delta x + \frac{1-a}{2a^2 x_0^2} \Delta x^2 + O(\Delta x^3) \right)$$

provides, with  $x_0 = M_a^a(S_t)$  and  $\Delta x = \Delta Y$ , the expression

$$\begin{aligned} M_a(S_{t+\Delta t}) &= M_a(S_t) + \frac{1}{dM_a^{a-1}(S_t)} \sum_{i=1}^d (S_t^i)^a \left( \mu^i \Delta t + \sigma^i \Delta B_t^{H^i} + \frac{a}{2} (\sigma^i)^2 (\Delta B_t^{H^i})^2 + O(\Delta t^2) + O(\Delta t \Delta B_t^{H^i}) \right) \\ &\quad + \frac{1-a}{2d^2 M_a^{2a-1}(S_t)} \sum_{i,j=1}^d (S_t^i S_t^j)^a \left( \sigma^i \sigma^j \Delta B_t^{H^i} \Delta B_t^{H^j} + \mathcal{J} \right), \end{aligned}$$

where  $\mathcal{J}$  collects all the remainder terms which, after taking expectation (see below), are of order  $o(\Delta t^{2H})$ . Substituting into (A.8), considering the definition of  $\mathcal{R}(t, a, \Delta t)$  in (A.9), and taking expectation supplies

$$\mathbb{E}[\mathcal{H}(t, a, \Delta t)] = \frac{a-1}{2d} \sum_{i=1}^d (\sigma^i)^2 \mathbb{E} \left[ \frac{(S_t^i)^a}{M_a^{a-1}(S_t)} \left( 1 - \frac{1}{d} \left( \frac{S_t^i}{M_a(S_t)} \right)^a \right) (\Delta B_t^{H^i})^2 \right] + o(\Delta t^{2H}).$$

Here, we have used the independence of the fBms  $B^{H^1}, \dots, B^{H^d}$  which implies that  $\mathbb{E}[\Delta B_t^{H^i} \Delta B_t^{H^j}] = 0$  for  $i \neq j$ . An application of Isserli's theorem similar to the proof of Proposition 3.2 in Appendix A.5 shows that all "mixed terms" ( $i \neq j$ ) in the double sum do not contribute to the leading term of the expansion. Another application of the theorem to the expectation on the r.h.s. yields

$$\mathbb{E}[\mathcal{H}(t, a, \Delta t)] = \frac{a-1}{2d} \sum_{i \in \mathcal{I}_{\min}} (\sigma^i)^2 \mathbb{E} \left[ \frac{(S_t^i)^a}{M_a^{a-1}(S_t)} \left( 1 - \frac{1}{d} \left( \frac{S_t^i}{M_a(S_t)} \right)^a \right) \right] \Delta t^{2H_{\min}} + o(\Delta t^{2H_{\min}}),$$

where we utilize the fact that the leading term of the expansion only collects the terms which are related to assets with the smallest Hurst coefficients, i.e.,  $H^i = H_{\min}$ . In view of (A.6), we have to evaluate sums of the form  $F = \sum_{n=1}^N \mathbb{E}[\mathcal{H}(t_{n-1}, a, \Delta t)]$  for which we obtain

$$\begin{aligned} F &= \sum_{n=1}^N \frac{a-1}{2d} \sum_{i \in \mathcal{I}_{\min}} \left\{ (\sigma^i)^2 \mathbb{E} \left[ \frac{(S_{t_{n-1}}^i)^a}{M_a^{a-1}(S_{t_{n-1}})} \left( 1 - \frac{1}{d} \left( \frac{S_{t_{n-1}}^i}{M_a(S_{t_{n-1}})} \right)^a \right) \right] \Delta t^{2H_{\min}} + o(\Delta t^{2H_{\min}}) \right\} \\ &= \frac{a-1}{2d} \frac{1}{\Delta t} \left\{ \int_0^T \mathbb{E} \left[ M_a(S_t) \sum_{i \in \mathcal{I}_{\min}} (\sigma^i)^2 \left( \frac{S_t^i}{M_a(S_t)} \right)^a \left( 1 - \frac{1}{d} \left( \frac{S_t^i}{M_a(S_t)} \right)^a \right) \right] dt + O(\Delta t) \right\} \times \\ &\quad \times (\Delta t^{2H_{\min}} + o(\Delta t^{2H_{\min}})) \\ &= \bar{C}(a) \Delta t^{2H_{\min}-1} + o(\Delta t^{2H_{\min}-1}). \end{aligned}$$

In this formulation, we consider the linear approximation order of the composite rectangular rule applied to the integral in the second line, and the definition of  $\bar{C}(a)$  in the proposition. Substituting the above expression into (A.6) leads to

$$\mathbb{E}[\mathcal{D}_T(\Delta t)] = \sum_{n=1}^N (\mathbb{E}[\mathcal{H}(t_{n-1}, \beta, \Delta t)] - \mathbb{E}[\mathcal{H}(t_{n-1}, \alpha, \Delta t)]) = (\bar{C}(\beta) - \bar{C}(\alpha)) \Delta t^{2H_{\min}-1} + o(\Delta t^{2H_{\min}-1}),$$

which proves the claim.  $\square$

## B Additional results

Figures B.1 and B.2 supply additional simulated realizations of the Salopek strategy to illustrate the effects of negative rebalancing costs and infinite strategy parameter values, respectively.

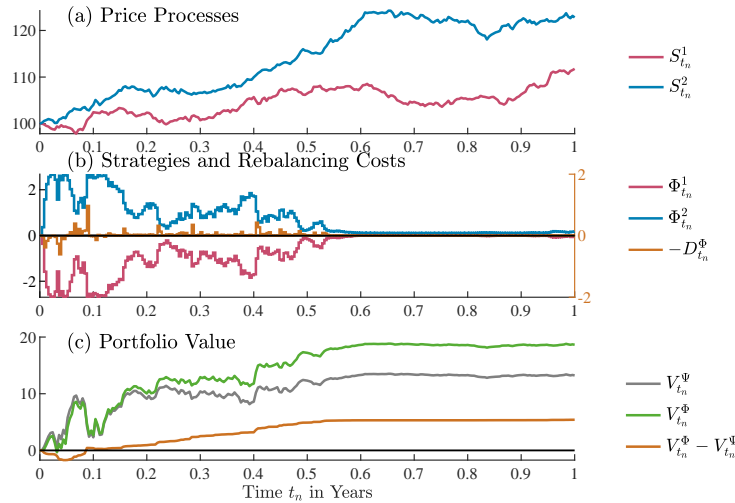
## C Alternative price model

In our main analysis, we have assumed that asset prices follow the fBm defined in (2.3). A straightforward alternative price model is the mixed fBm (mfBm). With simplified notation, i.e., after dropping the asset index  $i$ , it is given by

$$S_t = s_0 \exp \left\{ \mu t + \nu W_t - \frac{1}{2} \nu^2 t + \sigma B_t^H \right\}, \quad (\text{C.1})$$

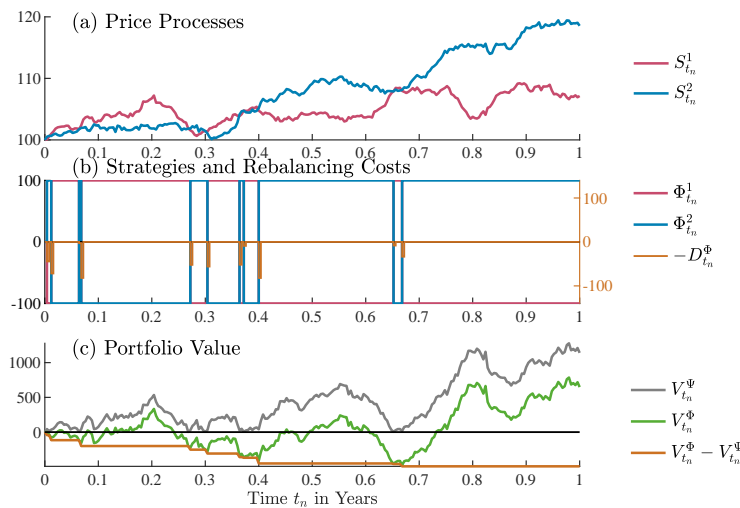
where  $W_t$  is a sBm and  $B_t^H$  represents a fBm with  $H > 0.5$ . Furthermore,  $W_t$  and  $B_t^H$  are independent and  $s_0, \sigma, \nu > 0, \mu \in \mathbb{R}$  (see Bender et al., 2011).

The fBm and the mfBm basically have the same covariance structure. That is, for  $H > 0.5$ , they both exhibit long range dependence controlled by  $H$ . However, the models differ with respect to their quadratic variation. While, in the case of  $H > 0.5$ , a fBm has zero quadratic variation, a mfBm displays the same positive quadratic variation as the sBm. This is important because our continuous-time arbitrage strategies require that the stock price model features zero quadratic variation (see Bender et al., 2008, 2011).



Using the overall design and setting of Figure 3.8, this figure simulates another exemplary realization of the Salopek strategy and replaces the  $(\alpha, \beta)$  basis values of  $(-30, 30)$  by  $(71, 80)$ .

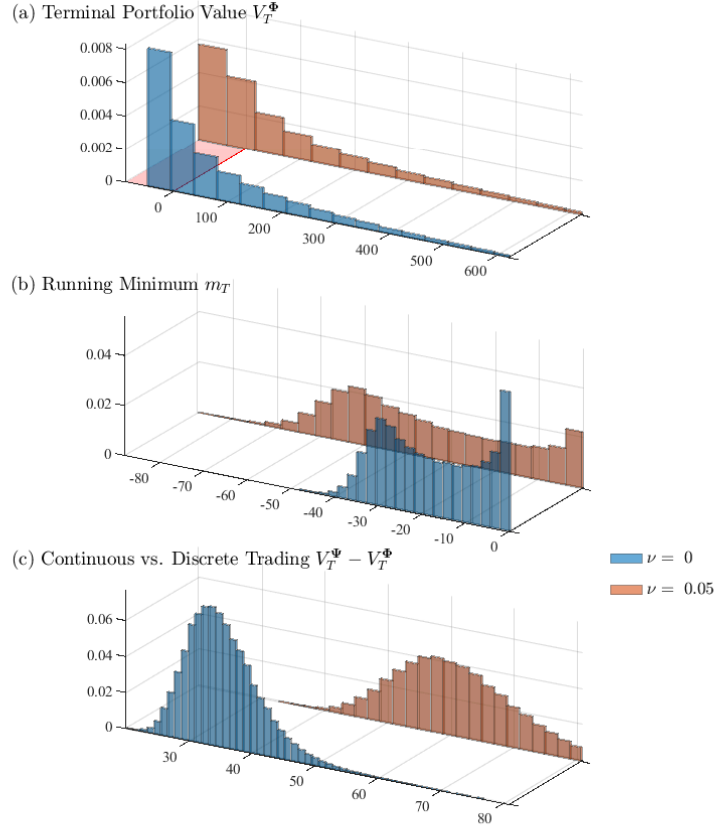
Fig. B.1: Realization of the discretized Salopek strategy with negative rebalancing costs



Using the simulated prices of Figure 3.8, this figure illustrates the behavior of the Salopek strategy in a situation where the  $(\alpha, \beta)$  basis values of  $(-30, 30)$  are replaced by  $(-\infty, \infty)$ .

Fig. B.2: Realization of the discretized Salopek strategy with parameter infinity

To see how our discretized strategies perform in the presence of positive quadratic variation, we repeat the simulations related to our basis setting (see Table 3.1) by generating mfBm prices instead of fBm prices. We start with a discussion of the merits of the Shiryaev strategy in a mfBm environment with  $\nu = 0.05$ . Following the style of Figure 3.2, Figure C.1 compares  $\nu = 0$  (fBm) to  $\nu = 0.05$  (mfBm). It shows that, even though the introduction of a small sBm component destroys the strategy's continuous-time arbitrage property, the discretized version of the trading rule can be useful because it generates a positive terminal value on average and extends the range of potential gains. However, as substantiated by the descriptive statistics of Table C.1, this comes at the cost of a higher loss probability. The additional  $\nu$  values covered by Table C.1 reveal that both the terminal mean and the loss probability rise with  $\nu$ . The latter increases drastically.



This figure reevaluates the basis setting results of the discretized Shiryaev strategy in Figure 3.2 by introducing a new price model, i.e., the mfBm specified in (C.1). While  $\nu = 0.05$  resembles a genuine mfBm,  $\nu = 0$  reduces the mfBm to a fBm. For better visibility, the x-axis in Panels (a) and (b) ends at the 95% quantile of  $\nu = 0.05$ .

Fig. C.1: Shiryaev portfolio value distributions for alternative price model

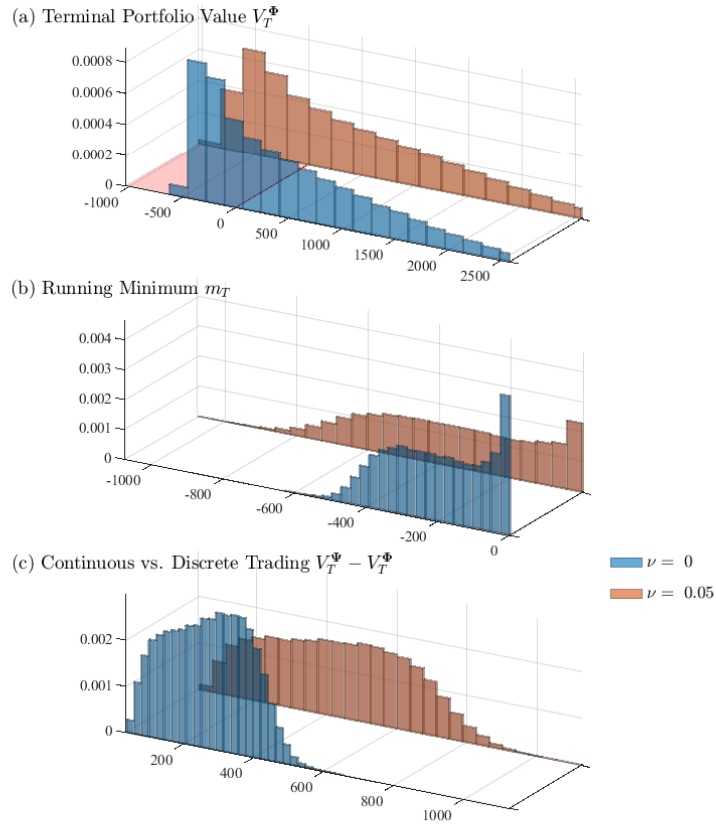
$\nu$	$H$	Mean	Median	Stand. dev.	Min	Max	Loss prob.
0.00	0.6	107.9	25.6	218.1	-48.2	4,148.5	0.39
0.05	0.6	111.3	11.6	266.5	-87.8	4,567.0	0.46
0.10	0.6	114.8	-31.7	406.2	-213.1	7,234.5	0.56
0.15	0.6	120.9	-104.2	651.1	-449.4	15,600.4	0.62
0.20	0.6	129.5	-203.4	1,020.8	-839.0	31,797.1	0.65
0.00	0.9	141.3	58.3	217.9	-1.8	3,764.9	0.06
0.05	0.9	145.3	44.7	268.7	-38.4	4,985.2	0.32
0.10	0.9	149.3	0.5	409.7	-146.9	7,299.8	0.50
0.15	0.9	156.1	-72.5	657.0	-362.9	13,721.6	0.59
0.20	0.9	165.7	-171.9	1,030.3	-691.4	26,376.8	0.63

Supplementing Figure C.1, this table reports some descriptive statistics for the terminal portfolio value distributions of the discretized Shiryaev strategy under the new price model (C.1) with  $\nu \in \{0, 0.05, 0.1, 0.15, 0.2\}$  and  $H \in \{0.6, 0.9\}$ .

Table C.1: Shiryaev portfolio value statistics for alternative price model

Turning to the Salopek strategy, Figure C.2 and Table C.2 indicate that, similar to the Shiryaev case, a mfBm increases the range of positive and negative terminal portfolio values. However, for the Salopek rule, a growing  $\nu$  lowers the terminal mean while simultaneously raising the loss probability. Nevertheless, in the considered  $\nu$  range, it remains beneficial for investors.





This figure reevaluates the basis setting results of the discretized Salopek strategy in Figure 3.9 by introducing a new price model, i.e., the mfBm specified in (C.1). While  $\nu = 0.05$  resembles a genuine mfBm,  $\nu = 0$  reduces the mfBm to a fBm. For better visibility, the x-axis in Panel (a) ends at the 95% quantile of  $\nu = 0.05$ .

Fig. C.2: Salopek sensitivity to strategy parameters for alternative price model

$\nu$	$H$	Mean	Median	Stand. dev.	Min	Max	Loss prob.
0.00	0.6	533.4	277.8	887.5	-625.6	6,454.2	0.37
0.05	0.6	495.4	215.7	1,056.7	-1,027.4	7,478.2	0.42
0.10	0.6	424.2	104.9	1,490.1	-2,313.9	9,766.3	0.47
0.15	0.6	365.3	15.4	2,071.9	-4,091.7	12,395.4	0.50
0.20	0.6	326.6	-58.3	2,731.2	-7,063.0	16,219.1	0.51
0.00	0.9	794.7	547.8	810.7	-18.2	6,752.4	0.07
0.05	0.9	717.3	443.4	995.5	-509.3	7,705.6	0.31
0.10	0.9	584.0	268.9	1,449.4	-1,855.2	9,813.8	0.43
0.15	0.9	480.9	130.2	2,044.6	-3,780.2	12,080.3	0.48
0.20	0.9	413.7	26.7	2,712.4	-6,384.2	16,651.3	0.50

Supplementing Figure C.2, this table reports some descriptive statistics for the terminal portfolio value distributions of the discretized Salopek strategy under the new price model (C.1) with  $\nu \in \{0, 0.05, 0.1, 0.15, 0.2\}$  and  $H \in \{0.6, 0.9\}$ .

Table C.2: Salopek portfolio value statistics for alternative price model

## References

- Amblard, P.O., Coeurjolly, J.F., Lavancier, F., Philippe, A., 2013. Basic properties of the multivariate fractional Brownian motion. *Séminaires & Congrès* 28, 65–87.
- Auer, B.R., 2016. Pure return persistence, Hurst exponents, and hedge fund selection: a practical note. *Journal of Asset Management* 17, 319–330.
- Auer, B.R., Schuhmacher, F., 2015. Liquid betting against beta in Dow Jones Industrial Average stocks. *Financial Analysts Journal* 71, 30–43.
- Badrinath, S.G., Gubellini, S., 2011. On the characteristics and performance of long-short, market-neutral and bear mutual funds. *Journal of Banking and Finance* 35, 1762–1776.
- Barroso, P., Santa-Clara, P., 2015. Momentum has its moments. *Journal of Financial Economics* 116, 111–120.
- Batten, J.A., Ciner, C., Lucey, B.M., Szilagyi, P.G., 2013. The structure of gold and silver spread returns. *Quantitative Finance* 13, 561–570.
- Bayraktar, E., Poor, H.V., 2005. Arbitrage in fractal modulated Black-Scholes models when the volatility is stochastic. *International Journal of Theoretical and Applied Finance* 8, 283–300.
- Bender, C., Sottinen, T., Valkeila, E., 2008. Pricing by hedging and no-arbitrage beyond semimartingales. *Finance and Stochastics* 12, 441–46.
- Bender, C., Sottinen, T., Valkeila, E., 2011. Fractional processes as models in stochastic finance, in: Nunno, G.D., Øksendal, B. (Eds.), *Advanced Mathematical Methods for Finance*, Springer, Berlin, Heidelberg. pp. 75–103.
- Bessembinder, H., 2018. Do stocks outperform Treasury bills? *Journal of Financial Economics* 129, 440–457.
- Biagini, F., Hu, Y., Øksendal, B., Zhang, T., 2008. *Stochastic Calculus for Fractional Brownian Motion and Applications*. Springer, London.
- Björk, T., 2004. *Arbitrage Theory in Continuous Time*. Oxford University Press, Oxford.
- Black, F., Scholes, M., 1973. The pricing of options and corporate liabilities. *Journal of Political Economy* 81, 637–654.
- Bodie, Z., Kane, A., Marcus, A.J., 2009. *Investments*. McGraw-Hill, New York.
- Bondarenko, O., 2003. Statistical arbitrage and securities prices. *Review of Financial Studies* 16, 875–919.
- Bouchaud, J.P., 2022. The inelastic market hypothesis: a microstructural interpretation. *Quantitative Finance* 22, 1785–1795.
- Brock, W., Lakonishok, J., LeBaron, B., 1992. Simple technical trading rules and the stochastic properties of stock returns. *Journal of Finance* 47, 1731–1764.
- Chamoli, A., Bansal, A.R., Dimri, V., 2007. Wavelet and rescaled range approach for the Hurst coefficient for short and long time series. *Computers and Geosciences* 33, 83–93.
- Chen, H.J., Chen, S.J., Chen, Z., Li, F., 2017. Empirical investigation of an equity pairs trading strategy. *Management Science* 65, 370–389.
- Cheridito, P., 2003. Arbitrage in fractional Brownian motion models. *Finance and Stochastics* 7, 533–553.
- Chordia, T., Subrahmanyam, A., Tong, Q., 2014. Have capital market anomalies attenuated in the recent era of high liquidity and trading activity? *Journal of Accounting and Economics* 58, 41–58.
- Coakley, J., Kellard, N., Wang, J., 2016. Commodity futures returns: more memory than you might think! *European Journal of Finance* 22, 1457–1483.
- Coeurjolly, J.F., 2000. Simulation and identification of the fractional Brownian motion: a bibliographical and comparative study. *Journal of Statistical Software* 5, 1–53.
- Cumova, D., Nawrocki, D., 2014. Portfolio optimization in an upside potential and downside risk framework. *Journal of Economics and Business* 71, 68–89.
- Cutland, N.J., Kopp, P.E., Willinger, W., 1995. Stock price returns and the Joseph effect: a fractional version of the Black-Scholes model, in: Bolthausen, E., Dozzi, M., Russo, F. (Eds.), *Seminar on Stochastic Analysis, Random Fields and Applications*, Springer, Berlin, Heidelberg. pp. 327–351.
- Danurdirdjo, D., Hirose, A., 2011. Synthesis of two-dimensional fractional Brownian motion via circulant embedding, in: *18th IEEE International Conference on Image Processing*. Institute of Electrical and Electronics Engineers, Brussels. pp. 1085–1088.
- Dasgupta, A., Kallianpur, G., 2000. Arbitrage opportunities for a class of Gladyshev processes. *Applied Mathematics and Optimization* 41, 377–385.

- Delbaen, F., Schachermayer, W., 1994. A general version of the fundamental theorem of asset pricing. *Mathematische Annalen* 300, 463–520.
- Di Cesare, A., Stork, P.A., De Vries, C.G., 2015. Risk measures for autocorrelated hedge fund returns. *Journal of Financial Econometrics* 13, 868–895.
- Dieker, A.B., Mandjes, M., 2003. On spectral simulation of fractional Brownian motion. *Probability in the Engineering and Informational Sciences* 17, 417–434.
- Dietrich, C.R., Newsam, G.N., 1997. Fast and exact simulation of stationary Gaussian processes through circulant embedding of the covariance matrix. *SIAM Journal on Scientific Computing* 18, 1088–1107.
- Du, S., Zhu, H., 2017. What is the optimal trading frequency in financial markets? *Review of Economic Studies* 84, 1606–1651.
- Eling, M., Schuhmacher, F., 2007. Does the choice of performance measure influence the evaluation of hedge funds? *Journal of Banking and Finance* 31, 2632–2647.
- Erb, C.B., Harvey, C.R., 2006. The strategic and tactical value of commodity futures. *Financial Analysts Journal* 62, 69–97.
- Frazzini, A., Pedersen, L.H., 2014. Betting against beta. *Journal of Financial Economics* 111, 1–25.
- Gao, G.P., Lu, X., Song, Z., 2018. Tail risk concerns everywhere. *Management Science* 65, 3111–3130.
- Garcin, M., 2022. Forecasting with fractional Brownian motion: a financial perspective. *Quantitative Finance* 22, 1495–1512.
- Goyal, A., Jegadeesh, N., 2018. Cross-sectional and time-series tests of return predictability: what is the difference? *Review of Financial Studies* 31, 1784–1824.
- Guasoni, P., 2006. No arbitrage under transaction costs, with fractional Brownian motion and beyond. *Mathematical Finance* 16, 569–582.
- Guasoni, P., Mishura, Y., Rásonyi, M., 2021. High-frequency trading with fractional Brownian motion. *Finance and Stochastics* 25, 277–310.
- Guasoni, P., Nika, Z., Rásonyi, M., 2019. Trading fractional Brownian motion. *SIAM Journal on Financial Mathematics* 10, 769–789.
- Hardy, G.H., Littlewood, J.E., Pólya, G., 1934. *Inequalities*. Cambridge University Press, Cambridge.
- Harrison, J.M., Pitbladdo, R., Schaefer, S.M., 1984. Continuous price processes in frictionless markets have infinite variation. *Journal of Business* 57, 353–365.
- Hassan, T.A., Mano, R.C., 2019. Forward and spot exchange rates in a multi-currency world. *Quarterly Journal of Economics* 134, 397–450.
- Hendricks, K.B., Singhal, V.R., 2005. An empirical analysis of the effect of supply chain disruptions on long-run stock price performance and equity risk of the firm. *Production and Operations Management* 14, 35–52.
- Hiemstra, C., Jones, J.D., 1997. Another look at long memory in common stock returns. *Journal of Empirical Finance* 4, 373–401.
- Hogan, S., Jarrow, R., Teo, M., Warachka, M., 2004. Testing market efficiency using statistical arbitrage with applications to momentum and value strategies. *Journal of Financial Economics* 73, 525–565.
- Hong, K.J., Satchell, S., 2015. Time series momentum trading strategy and autocorrelation amplification. *Quantitative Finance* 15, 1471–1487.
- Hu, Y., Øksendal, B., 2003. Fractional white noise calculus and applications to finance. *Infinite Dimensional Analysis, Quantum Probability and Related Topics* 6, 1–32.
- Jegadeesh, N., Titman, S., 1993. Returns to buying winners and selling losers: implications for stock market efficiency. *Journal of Finance* 48, 65–91.
- Jegadeesh, N., Titman, S., 2001. Profitability of momentum strategies: an evaluation of alternative explanations. *Journal of Finance* 56, 699–720.
- Karemera, D., Kim, B.J.C., 2006. Assessing the forecasting accuracy of alternative nominal exchange rate models: the case of long memory. *Journal of Forecasting* 25, 369–380.
- Kijima, M., Tam, C.M., 2013. Fractional Brownian motions in financial models and their Monte Carlo simulation, in: Chan, V.W.K. (Ed.), *Theory and Applications of Monte Carlo Simulations*. IntechOpen, Rijeka, pp. 53–85.
- Krauss, C., 2017. Statistical arbitrage pairs trading strategies: review and outlook. *Journal of Economic Surveys* 31, 513–545.
- Kristoufek, L., 2012. How are rescaled range analyses affected by different memory and distributional properties? A Monte Carlo study. *Physica A: Statistical Mechanics and its Applications* 391, 4252–4260.

- Kroese, D.P., Botev, Z.I., 2015. Spatial process simulation, in: Schmidt, V. (Ed.), *Stochastic Geometry, Spatial Statistics and Random Fields*. Springer, Basel, pp. 369–404.
- Lin, S.J., 1995. Stochastic analysis of fractional Brownian motions. *Stochastics and Stochastics Reports* 55, 121–140.
- López-Garíca, M.N., Trinidad-Segovia, J.E., Sánchez-Granero, M.A., Pouchkarev, I., 2021. Extending the Fama and French model with a long term memory factor. *European Journal of Operational Research* 291, 421–426.
- Lütkebohmert, E., Sester, J., 2019. Robust statistical arbitrage strategies. *Quantitative Finance* 21, 379–402.
- Malcenièce, L., Malcenièks, K., Putniņš, T.J., 2019. High frequency trading and comovement in financial markets. *Journal of Financial Economics* 134, 381–399.
- Mandelbrot, B.B., Ness, J.W.V., 1968. Fractional Brownian motions, fractional noises and applications. *SIAM Review* 10, 422–437.
- Marshall, B.R., Nguyen, N.H., Visaltanachoti, N., 2017. Time series momentum and moving average trading rules. *Quantitative Finance* 17, 405–421.
- Mehlitz, J.S., Auer, B.R., 2024. Memory-enhanced momentum in commodity futures markets. *European Journal of Finance* 30, 773–802.
- Michalowicz, J.V., Nichols, J.M., Bucholtz, F., Olson, C.C., 2009. An Isserlis’ theorem for mixed Gaussian variables: application to the auto-bispectral density. *Journal of Statistical Physics* 136, 89–102.
- Mishura, Y.S., 2008. *Stochastic Calculus for Fractional Brownian Motion and Related Processes*. Springer, Berlin, Heidelberg.
- Moskowitz, T.Y., Ooi, Y.H., Pedersen, L.H., 2012. Time series momentum. *Journal of Financial Economics* 104, 228–250.
- Nascimento, J., Powell, W., 2010. Dynamic programming models and algorithms for the mutual fund cash balance problem. *Management Science* 56, 801–815.
- Pan, M.S., Liano, K., Huang, G.C., 2004. Industry momentum strategies and autocorrelations in stock returns. *Journal of Empirical Finance* 11, 185–202.
- Peyre, R., 2017. Fractional Brownian motion satisfies two-way crossing. *Bernoulli* 23, 3571–3597.
- Rachev, S., Jašić, T., Stoyanov, S., Fabozzi, F.J., 2007. Momentum strategies based on reward-risk stock selection criteria. *Journal of Banking and Finance* 31, 2325–2346.
- Rogers, L.C.G., 1997. Arbitrage with fractional Brownian motion. *Mathematical Finance* 7, 95–105.
- Rostek, S., Schöbel, R., 2013. A note on the use of fractional Brownian motion for financial modeling. *Economic Modelling* 30, 30–35.
- Salopek, D.M., 1998. Tolerance to arbitrage. *Stochastic Processes and their Applications* 76, 217–230.
- Schuhmacher, F., Eling, M., 2011. Sufficient conditions for expected utility to imply drawdown-based performance rankings. *Journal of Banking and Finance* 35, 2311–2318.
- Shiryaev, A.N., 1998. On arbitrage and replication for fractal models. MPS Working Paper No. 1998-20.
- Sikora, G., 2018. Statistical test for fractional Brownian motion based on detrending moving average algorithm. *Chaos, Solitons and Fractals* 116, 54–62.
- Simutin, M., 2014. Cash holdings and mutual fund performance. *Review of Finance* 18, 1425–1464.
- Sottinen, T., Valkeila, E., 2003. On arbitrage and replication in the fractional Black-Scholes pricing model. *Statistics and Decisions* 21, 93–107.
- Stein, M.L., 2002. Fast and exact simulation of fractional Brownian surfaces. *Journal of Computational and Graphical Statistics* 11, 587–599.
- Wang, X.T., Wu, M., Zhou, Z.M., Jing, W.S., 2012. Pricing European option with transaction costs under the fractional long memory stochastic volatility model. *Physica A: Statistical Mechanics and its Applications* 391, 1469–1480.
- Weron, R., 2002. Estimating long-range dependence: finite sample properties and confidence intervals. *Physica A: Statistical Mechanics and its Applications* 312, 285–299.
- Wilcox, D., Gebbie, T., 2008. Serial correlation, periodicity and scaling of eigenmodes in an emerging market. *International Journal of Theoretical and Applied Finance* 11, 739–760.
- Willinger, W., Taqqu, M.S., Teverovsky, V., 1999. Stock market prices and long-range dependence. *Finance and Stochastics* 3, 1–13.
- Wood, A.T.A., Chan, G., 1994. Simulation of stationary Gaussian processes in  $[0,1]^d$ . *Journal of Computational and Graphical Statistics* 3, 409–432.
- Xiang, Y., Deng, S., 2024. Statistical arbitrage under a fractal price model. *Annals of Operations Research* 335, 425–439.

- Yin, Z.M., 1996. New methods for simulation of fractional Brownian motion. *Journal of Computational Physics* 127, 66–72.
- Zakamulin, V., Giner, J., 2024. Optimal trend-following rules in two-state regime-switching models. *Journal of Asset Management* 25, 327–348.